Lucie Kubínová
Jana Albrechtová

STEREOLOGY in PLANT ANATOMY

Prague, 28 June – 2 July 1999

Adjoining International Course to the Conference S⁴G

Department of Plant Physiology, Charles University in Prague

Corporate Sponsor:

OLYMPUS

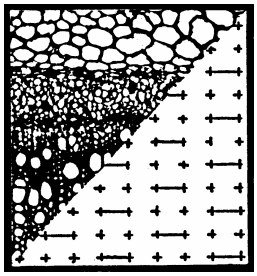

Title:

STEREOLOGY IN PLANT ANATOMY

Authors:
Dr. Lucie Kubínová[2*], Dr. Jana Albrechtová[1**]

Textbook to the International Course on Stereology in Plant Anatomy
(Prague, CZ, 28 June – 2 July 1999)

Adjoining International Course to the International Conference S^{4}G
"Stereology, Spatial Statistics and Stochastic Geometry"
(Prague, CZ, 21 June – 24 June 1999)

Under the auspices of:
Academy of Sciences of the Czech Republic,
Faculty of Science of Charles University in Prague, and
Royal Microscopical Society

Corporate Sponsor:
OLYMPUS

Venue:
[1]Department of Plant Physiology, Faculty of Science, Charles University, Vinicná 5, 128 44, Prague 2
[2]Department of Biomathematics, Institute of Physiology, Vídenská 1083, 142 20 Prague 4
* e-mail: kubinova@sun1.biomed.cas.cz
** e-mail albrecht@natur.cuni.cz

Lecturers:
Dr. Jana Albrechtová[1], Dr. Lucie Kubínová[2], Dr. Jirí Janácek[2], Dr. Olga Votrubová[1]

Honorary lecturers:
Dr. C. Vyvyan Howard
Representative of the Royal Microscopical Society, University of Liverpool, UK
Dr. Zdenek Opatrný
Head of the Department of Plant Physiology, Faculty of Science, Charles University, CZ

Charles University, 1999.

CONTENT

INTRODUCTION

This textbook was written for the attendants of the Course on Stereology in Plant Anatomy, held in Prague, at the Department of Plant Physiology, Faculty of Science, Charles University and in the Institute of Physiology, Academy of Science of the Czech Republic (AS CR), from 28 June to 2 July 1999.

The aim of this textbook is to present the principles of a number of morphometrical methods leading to the estimation of plant anatomical characteristics, with a special stress on the unbiased stereological methods. An attempt was made to describe the methods in an easy-to-follow manner while their theoretical background was reduced to a minimum. The readers wishing to get a better knowledge of the theory are referred to the references.

Firstly, the measurements in two-dimensional space (2D), i.e. plane, are described - estimation of linear characteristics, area, curve length in 2D, and number of 2D particles. Some of these procedures are exploited in the quantitative evaluation of 3-dimensional (3D) structure. Selection of unbiased stereological methods for the estimation of volume density, volume, number, mean cell volume, surface area and curve length in 3D are then presented. For majority of methods technical and practical considerations of the implementation are discussed. The importance of correct and efficient sampling design is discussed in the end of the textbook.

Currently, image analysis (IA) is more and more often commonly used for quantification of structural parameters. In addition to characterization of planar and shape characteristics IA allows evaluation of the intensity of an observed colour and comparison of optical densities of different colours. However, without application of stereological principles it cannot give the information about spatial parameters and still not all laboratories are equipped with this expensive system. In the Module I we focus on giving other alternative ways of measurements in 2D without using sophisticated equipment but still obtaining reliable estimations. The Module II gives a review of stereological methods aimed at estimation of 3-D parameters, which cannot be obtained by only application of tools of image analysis. But these methods can be employed during image analysis processing greatly enlarging its application potential. This will be demonstrated on the software systems for generating stereological grids on a digital image of studied anatomical structures C.A.S.T. GRID Olympus; STESYS Institute of Physiology AS CR).

1. MODULE I: Morphometric Measurements in 2D

1.1. Estimation of linear characteristics

1.1.1. Measurements of linear characteristics

Linear characteristics of biological structures present in plant microscopic specimens are measured using a ruler. This can be done either in microscope using an ocular ruler which is inserted into the eyepiece of the microscope or on photographs when knowing magnification of them. When measuring length we superimpose the ruler in a manner to comprise the measured length of the measured object (Fig. 1, 2). The important step leading to good length estimation is calibration of a ruler (see Section 1.1.2.). Also in case we want to determine a mean length of some structure having a high abundance in observed object (e.g. stomata in epidermis) it is necessary to select representative set of measured structures. The principle of sampling in such case is given in the Section 1.4.1.

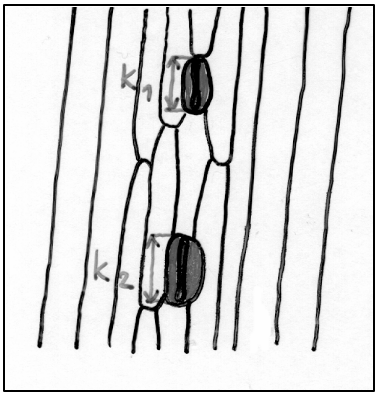

Fig. 1: Measurements of stoma length ***k***

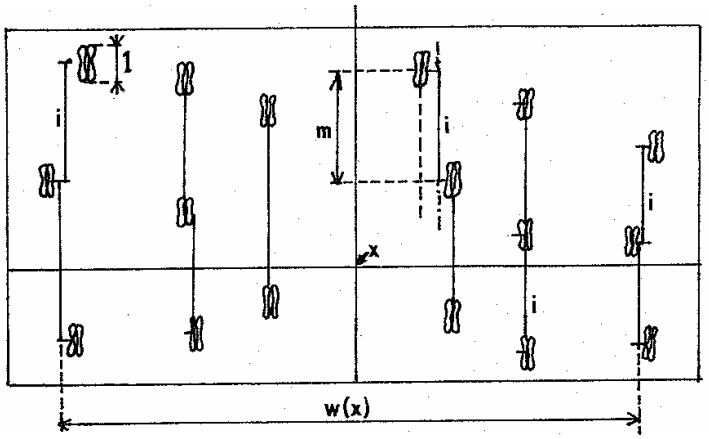

Fig. 2: Measurements on grass epidermis: stoma length ***l,*** distance ***m*** between stomata in one row, mean distance ***p*** between rows of stomata measured as a distance ***w(x)*** between ***n*** rows, then calculated as ***p = w(x) / n***

1.1.2. Practical examples of linear measurements in plant anatomy:

- **epidermal quantitative characteristics** (Fig. 1, 2): stoma length, for grass leaves distance between stomata in one row, mean distance between rows of stomata
- **diameter of root metaxylem vessels** (Fig. 3)
- **height and width of an apical meristem**

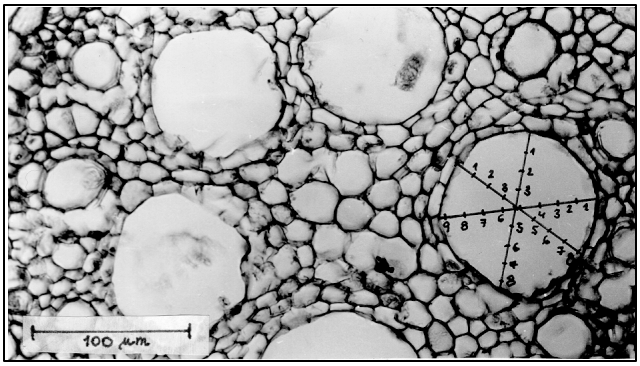

Fig. 3: Diameter of root metaxylem vessels (maize): when measuring the diameter of not completely circular objects it is recommended to measure a distance from several directions, e.g. shifted by 30°. A diameter is then the average of these 3 measurements.

1.1.3. Calibration of a ruler

When estimating length characteristics the calibration must be performed, i.e. the actual length of one unit of a ruler must be determined. We explain the principle on calibration of an ocular ruler, which is probably the most complicated example of calibration. The ocular ruler usually consists of a scale 10 mm long, divided into 100 units, each having the length of 100 µm. Firstly, a magnification convenient for the measurements of the structure under study is chosen.

Calibration is then done with the help of an objective micrometer (glass slide with a scale 1 mm long divided into 100 segments, each having the length of 10 µm). The view into the ocular containing an ocular ruler simultaneously with inserted objective micrometer is given in Fig. 4.

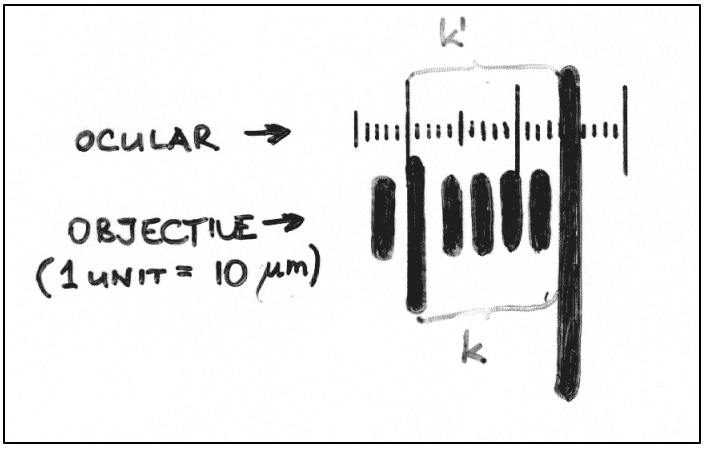

Fig. 4: Calibration: A view into the ocular containing an ocular ruler simultaneously with observed objective micrometer. Ocular ruler is less magnified than objective micrometer. Thus we abstract thicker lines of objective micrometer as 1-dimensional boundary lines from 1 side. Then we count coinciding lines of ocular ruler k' with boundary lines of objective micrometer k.

If k segments of the objective micrometer coincide with k' segments of the ocular ruler, then the length of one segment of the ocular ruler is equal to (k/k') x 100 µm. Therefore, if the linear dimension of the structure (e.g. length, width, diameter) corresponds to K segments of the ocular micrometer, than its actual value is K x (k/k') x 100 µm .

That means all our obtained linear characteristics are in relative units of length before calibration and to obtain actual values they must be multiplied by a calibration coefficient, which says what is an actual length of a ruler used. The calibration of the ocular ruler is clearly dependent on the magnification, therefore it must be determined for each magnification separately.

1.1.4. Measurements with n-class ruler

Less frequently used but usually more efficient way of measurement of mean linear characteristics (e.g. mean stoma length, mean diameter of vessels, length of somatic embryos), using the ruler with a very low number of segments, is described below.

The application of n-class ruler (see, e.g. Gundersen et al., 1981) (which can be inserted in the eyepiece of the microscope and calibrated analogously as described in Section 1.1.3.) is demonstrated by the example of the measurement of the mean stoma length (Fig.5). The lengths of stomata are classified into n size classes (n=6 in Fig.5) according to the following rule: the given length belongs to the k-th class if it is larger than $k-1$ intervals of the ruler and smaller than or equal to the length of k intervals.

The mean stoma length $\bar{l}(st)$ then can be calculated by using the formula:

$$\bar{l}(st) = \frac{1}{m} \cdot \sum_{k=1}^{n} m_k \cdot (k - \frac{1}{2}) \cdot l(\text{int}) \qquad (1)$$

where n is the total number of size classes of the ruler, m_k is the number of lengths belonging to the *k*-th class, m is the total number of lengths (i.e. $m = m_1 + m_2 + ... + m_n$) and l(int) is the actual length of one interval of the ruler (it is determined during the calibration procedure).

The measurement using *n*-class ruler is usually quicker than the one using the ruler consisting of a large number of 100 or more segments while its precision can be high enough - around ten size classes are usually sufficient.

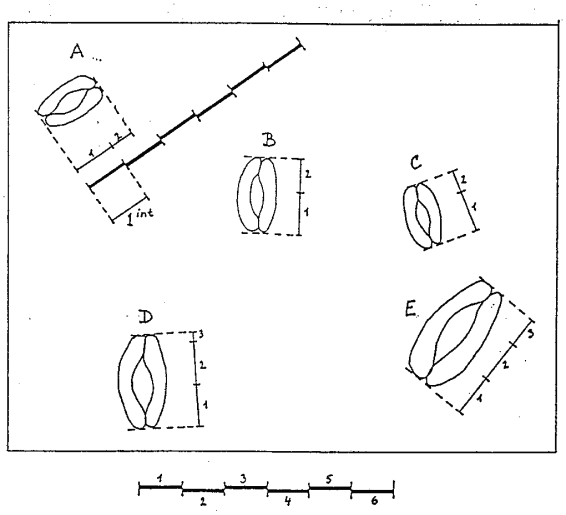

Fig.5. Measurement of linear characteristics using n-class ruler. The implementation of 6-class ruler (i.e. n=6) is shown:

Stomata A, B, C belong to the 2nd class and stomata D, E to the 3rd class, hence m_1=0, m_2=3, m_3=2, m_4=m_5=m_6=0 and so m=3+2=5. It means that, if l(int)=0.02 mm, the mean stoma length is equal to 0.038 mm = 38 µm:

l(st) = 1/5 x (3 x 3/2 + 2 x 5/2) x 0.02 =
= 19/10 x 0.02 = 0.038 mm

1.1.5. Practical considerations when estimating linear characteristics

A projection screen, if available, can make the linear measurements easier. The measurement procedure is analogous to the one described above while the ruler is attached to the projection screen instead of being inserted into the eyepiece.

A convenient way is to use a computer-assisted approach when the image is displayed by a camera on a screen and the length measurements can be done interactively by clicking a mouse using a relevant image analysis software.

Sometimes, it is advantageous to perform the measurements on the photographs. In this case it is recommended to record magnification used or to take a photograph of an objective micrometer immediately after photographing the studied structure so the calibration can then be made easily.

1.1.6. Making your own ocular ruler or test system

The ocular rulers can be easily made according to our own choice, by drawing the grid on a paper enough magnified and digitalization of the picture by a camera (or scanner) when leaving enough large margins. A field of a developed film (or photoreproduction on durable transparent positive film) is then cut into circle containing your grid with a diameter fitting into the ocular of your microscope. (Note different microscopes have different diameter of their oculars). Also good xerox-copying with desirable resolution could do the same job.

1.2. Area estimation

1.2.1. Review of methods

There is a number of methods for the measurement of the area of structures (microscopical as well as macroscopical ones), e.g. leaf area, the area of stomatal apertures measured from the replicas of the leaf epidermis or the area of vessel sections in a root. Let us mention some of them. Currently the most used method of area estimation is image analysis. Particularly when measured objects have a distinct boundary, which is distinguishable on the base of a different colour when compared with their background. The area of structures can be also measured by a digitizer (e.g. Parker and Ford, 1982, Harris et al., 1981), which requires manual tracing of structure contours. When computer-aided equipment is not available or object segmentation is not achieved in image pre-processing, other methods can be employed including morphometric methods.

Formerly, several methods were used. The measurements of the area of microscopical structures were most frequently based on the manual tracing or photographing of the outline of microscopical image of these structures. The area was then often measured by a planimeter (e.g. Turrell, 1936) or by a method consisting of cutting out the structure drawing or photograph and weighing it (e.g. El-Sharkawy & Hesketh, 1965, Charles-Edwards et al., 1972, Dengler & MacKay, 1975). The actual area of the structure was then calculated by the ratio of the measured area to the magnification used. Other method consisted in the tracing of the structure contours to a graph paper and subsequent counting of graph paper squares (1 square unit = 1 mm^2) lying entirely or by more than a half of their area inside the structure.

1.2.2. Morphometric methods: point-counting method and method of linear integration

Morphometric methods based on design, namely the point-counting and linear integration methods, are used less frequently, yet they do not require any expensive equipment or the laborious tracing of structure contours, which makes them very efficient.

When using the linear integration method (Weibel, 1979, p.27) a test system of parallel lines, placed systematically at the constant distance d, is superimposed on the structure under study. Lengths of the intersections of these lines with the structure are measured (see Fig.6) and the area (A) of the structure is estimated by the formula:

$$estA = L \cdot d \qquad (2)$$

where L is the total length of the intersections of the test lines with the structure and d is the distance between test lines. (*est A* denotes the estimate of parameter A; for further explanation see Section II.2.).

When using the point-counting method (Weibel, 1979, p.28) a point test system is superimposed on the structure (see Fig. 7). The points hitting the structure are counted and the area (A) of the structure is estimated by the formula:

$$estA = P \cdot a \qquad (3)$$

where P is the number of test points hitting the structure and a is the (actual) area unit corresponding to one test point of the test system (see Fig.7).

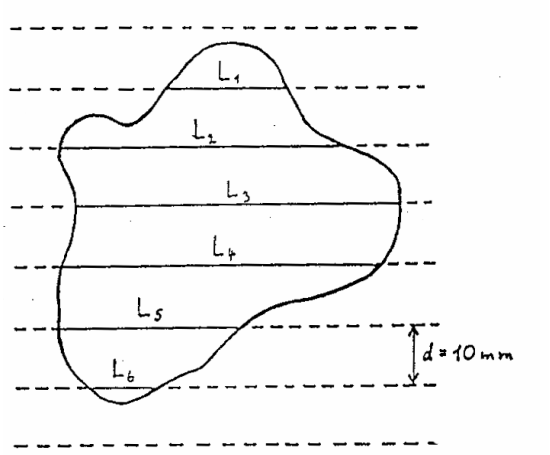

Fig. 6: Estimation of area (A) by the linear integration method:

est A = L . d = (L_1 + L_2 + L_3 + L_4 + L_5 + L_6) . d =
= (21 + 48 + 55 + 54 + 30 + 10) . 10 = 2180 (mm^2)

The area estimate is 21.8 cm^2 here.

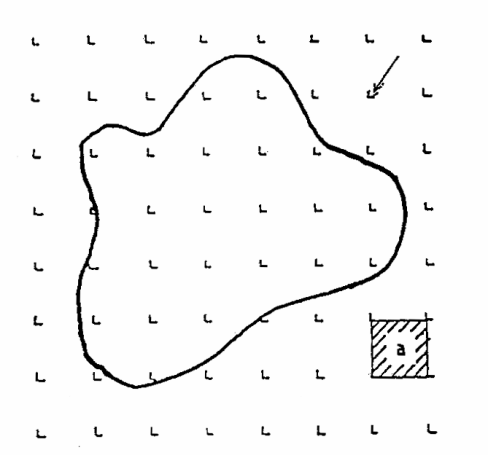

Fig. 7: Estimation of area (A) by the point-counting method.

est A = P . a = 22 . 100 = 2200 (mm^2),

here a (=100 mm^2) is the area corresponding to one test point. (Test points are the intersection points of the short lines.) The area estimate is 22 cm^2 here.

1.2.3. Principle of systematic uniform random superimposition of test system

In order to get unbiased area estimates, the test systems of lines or points must be superimposed on the structure uniformly at random (see Fig. 8).

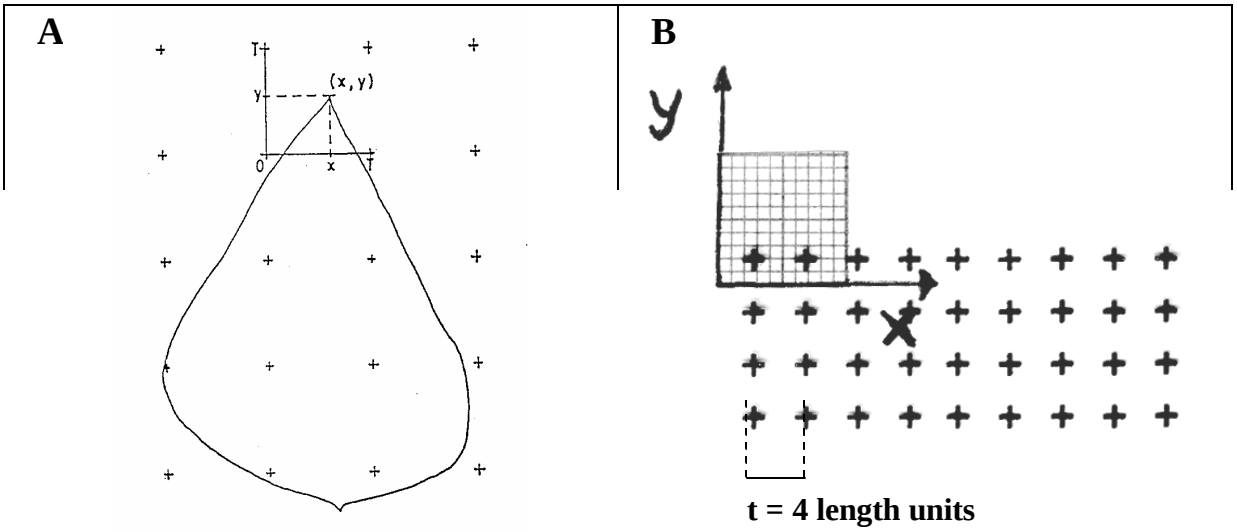

Fig. 8: Uniform random position of the point grid

A) **Superimposition on an object with defined point (e.g. leaf tip).**The distance (T) (mm) between the points of the grid is chosen first. Numbers x and y are then selected at random from the set {0,1,...,T-1}. The uniform random position of the point grid is ensured by placing the leaf tip in the position (x,y).

B) **Example of random superimposition of a test grid using an orienting 1mm grid.** The distance between two test points t = 4 length units. Thus, we select numbers x and y random from the set {0,1,2,3}, e.g. 3 and 2. The uniform random position of the point grid is ensured by placing 1 point of test grid in the position (x,y)= (3,2).

When using the point-counting method, it is recommended to use systematic point test systems rather than randomly distributed test points (Fig. 9) because of much higher efficiency of systematic sampling (Gundersen and Jensen, 1987).

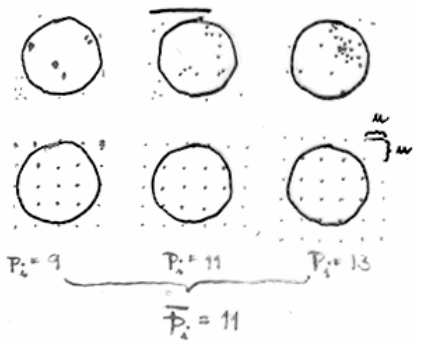

Fig. 9: Comparison of efficiency of differently arranged point-test systems

A) with randomly distributed points and,
B) with systematically distributed test points. Random superimposition of systematic point-test system does not affect the efficiency. P_I is a number of points hitting the structure, u is the length of one side of the square belonging to one point of the point test system.

1.2.4. Practical considerations of the morphometric method implementation

Both methods regarding their accuracy are similarly efficient. Generally, when we are deciding which one to use, we consider a shape of a measured structure and how much it is broken. For more compact and large structures linear integration method could be faster, for more broken structures point-counting method is faster than the linear integration one.

In general, the point-counting method proves to be the most efficient method of area estimation in biological research (see Weibel, 1979, Gundersen et al., 1981, Mathieu et al., 1981). Only the method using automatic image analysis can be quicker but it requires automatic recognition of structures under study which is not possible in the case of many types of biological structures. A number of studies (e.g. Gundersen et al., 1981) showed that point counting leads to a sufficiently precise result far more quickly then any method based on manual tracing of contours of the structures. Moreover, the point-counting method can be performed directly in the microscope with an appropriate ocular point test system, which can be inserted into the eyepiece of the microscope and so the measurements can be made directly in the microscope without the necessity of making any drawings or photographs (ocular test systems can be made as described in Section 1.1.6.).

A projection screen, if available, can be very useful also for the application of the point-counting method. In this case the point test system is attached directly to the screen. A computer-assisted approach can be very convenient if a special software for displaying the test system over the evaluated image is available, e.g. CAST-Grid (Olympus, Denmark), Digital Stereology (Kinetic Imaging Ltd, UK), STESYS (Karen et al., 1998).

1.3. Estimation of curve length in 2-D

1.3.1. Review of methods

Quite often in analysis of plant structure we need to determine curve length in 2D (e.g. vein length in a leaf, perimeter of cell sections in a planar section of a plant organ, length of extraradical mycelium of micorrhiza).

Currently method of estimation of curve length in 2D frequently used is image analysis. Particularly when measured objects have a distinct boundary, which is distinguishable on the base of different colour when compared with their background.

Traditional methods of the measurement of curve length are based on the curve tracing by a curvemeter or on the usage of a scribing-compass. These methods are time-consuming and can be biased, e.g. by the unprecise tracing of curves. The more recent methods using the digitizer, which also requires manual tracing of curves, is also time-consuming and brings the danger of an operator-dependent bias (Barba et al., 1992).

1.3.2. Morphometric methods: line-intercept method (Buffon method)

1.3.2.1. Curve length per area unit (curve density)

In general, if image analysis cannot be applied, more efficient way of estimation of the curve length in 2-D than traditional methods can offer, is the use of a stereological method called the **line-intercept method or Buffon method** (Weibel, 1979, p.33). A system of test lines is superimposed on the 2-D structure under study (e.g. cleared flat leaf with visible veins) and the intersections of test lines with the curves (e.g. veins) are counted (see Fig. 10**).** The length of curves per unit area of the structure (B_A) (e.g. vein density) is then estimated by the formula:

$$estB_A = \frac{p}{2} \cdot \frac{I}{L} \qquad (4)$$

where I is the number of intersection points between the curves and test lines and L is the total length of the parts of test lines lying in the structure (it is the actual length and so the calibration should be done as shown in Section 1.1.3.) (π is Ludolf's number, π = 3.14159...). Note that B_A is expressed in units of length (e.g. mm) per units of area (e.g. mm^2), i.e. mm^{-1}.

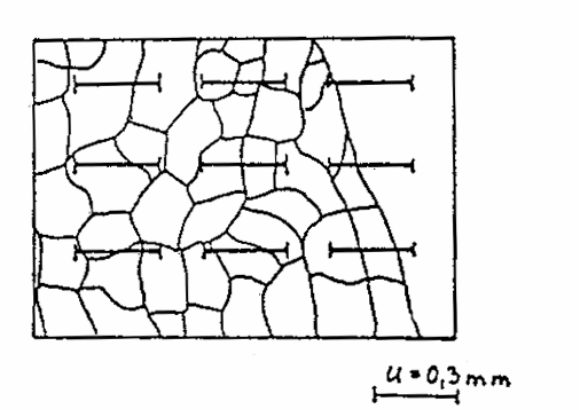

Fig.10: The estimation of vein density (B_A) using test system of combination of test lines and using formula (4).
A system of test lines is superimposed on the leaf with visible veins. I = 13, L = 7.2 x u = 7.2 x 0.3 = 2.2 (mm) here and so the estimate of vein density is 9.3 mm^{-1} here, i.e.

$$est\ B_A = \frac{p}{2} \cdot \frac{13}{2.2} = 9.3\ (mm^{-1})$$

Counting points is easier than length measurements and so the following modification of the Buffon method is most frequently used: A system of test lines and points is superimposed on the 2-D structure under study (see Fig.11) and the following formula used:

$$estB_A = \frac{p}{2} \cdot \frac{p}{l(t)} \cdot \frac{I}{P} \qquad (5)$$

where I is the number of intersection points between the studied curves and test lines, $p/l(t)$ is the ratio of the total number of test points to the total actual length of test lines in the test system used (it

is a constant number for a given test system and magnification) and *P* is the number of test points falling in the 2-D structure.

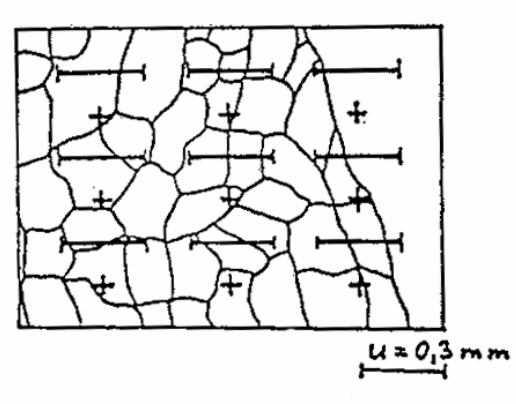

Fig.11: The estimation of vein density (B_A) using test system of combination of test lines and points and using formula (5).
A system of test lines and points is superimposed on the leaf.

I = 13, P = 8, p/l(t) = 9/9 x 1/u = 3.3 mm^{-1},

i.e. $estB_A = \frac{p}{2} \times 3.3 \times \frac{13}{8} = 8.4(mm^{-1})$

The estimate of vein density is 8.4 mm^{-1} here.

1.3.2.2. Total curve length in 2D

The total length of curves in 2D (e.g. root length, length of mycelium) can be easily calculated by multiplying B_A from formula 4 by the structure area (estimated, e.g., by the point-counting method, see Section I.2.). For example, the vein length B in a leaf can be calculated by the product of the corresponding vein density and leaf area. The root length (Fig. 12) is calculated similarly, by the formula

$$estB = \frac{p}{2} \cdot \frac{I}{L} \cdot A \qquad (6)$$

where *I* is the number of intersection points between the root and test lines and *L* is the total length of the parts of test lines comprising the structure which correspond to the area comprising the structure (it is the actual length and so the calibration should be done as shown in Section 1.1.3.), A is the area of test system comprising the structure measured.

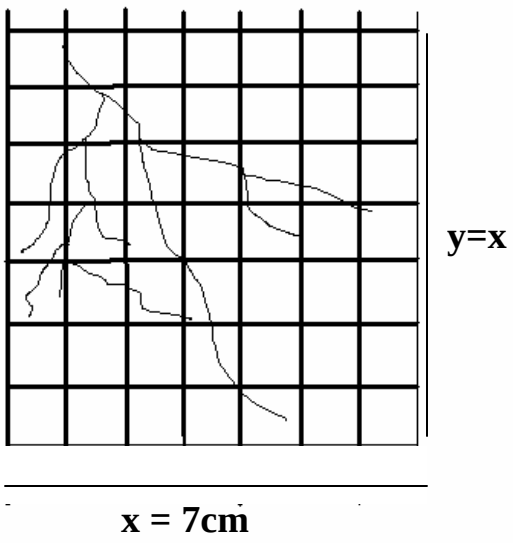

Fig. 12: Estimation of root length using the line intercept method.
I=23, L is the length of all thick test lines within the area comprising the structure, i.e. y.7cm + x . 7cm , i.e. 49 + 49 = 98 cm and A is area obtained as a product x . y = 49 cm^2. The root length B is 18 cm here.

$$estB = \frac{p}{2} \cdot \frac{I}{L} \cdot A$$

$$est\,B_A = \frac{p}{2} \cdot \frac{23}{98} \cdot 49 = 18\ cm$$

1.3.2.3. Practical considerations of the use of the line intercept method

When we want to apply the line intercept method we must consider the arrangement of measured structure. Isotropic arrangement is such, which has no preferential orientation in a plane whilst anisotropic structure has preferential orientation of its arrangement (Fig. 13). The formulas (4) (5) and (6) are valid for isotropic curves (i.e.), when the test lines may be of any shape or orientation. Usually it is convenient then to use anisotropic test system composed of parallel lines or squares. When structure is anisotropic, such as venation of monocotyledonous leaves, isotropic test system must be used, e.g. composed of quarter-circle arcs. Fig. 14 shows a combination of isotropic and anisotropic test system.

We should keep in mind that test systems must be superimposed on the structure uniformly at random (see Fig. 8). Again, a suitable ocular test system can be used for the application of the mentioned stereological methods (see Section 1.1.4.).

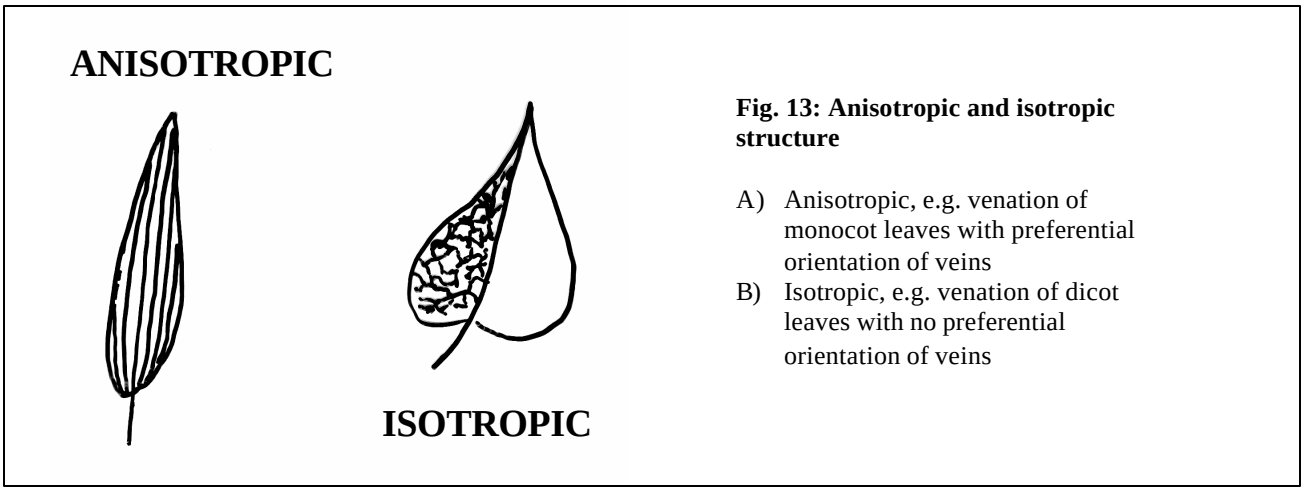

Fig. 13: Anisotropic and isotropic structure

A) Anisotropic, e.g. venation of monocot leaves with preferential orientation of veins
B) Isotropic, e.g. venation of dicot leaves with no preferential orientation of veins

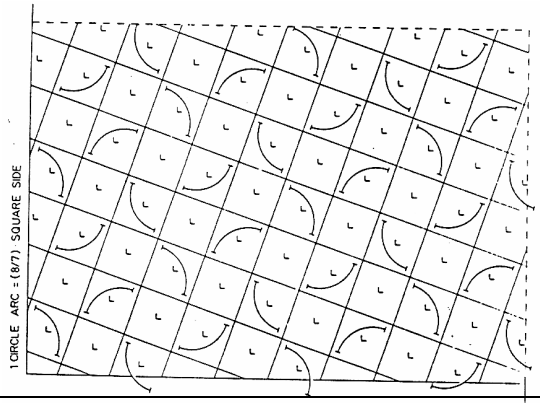

Fig. 14: Combination of isotropic (circle arcs) and anisotropic (lines) test systems and point grid

From Cruz-Orive and Hunziker ,1986)

1.4. Counting and sampling of 2-D particles

1.4.1. Principle of the method

When estimating the number of two-dimensional particles, some of the particles are usually sampled by sampling frames of some kind (following some kind of a sampling rule) from the entire population of particles under study. The sampled particles are then counted. In the plant anatomy context, the examples of two-dimensional particles are replicas of stomata or ordinary epidermal cells (or their projections from strips of the leaf epidermis). The rule of sampling particles by the

frames should ensure their unbiased sampling what means that each particle would have the same probability to be sampled. For example, in the case of stomata sampling the following condition must be fulfilled: If the entire leaf surface were covered by sampling frames (lying side by side but not intersecting each other), then every stoma should be sampled by one and only one frame. The sampling frame with extended full-drawn exclusion-edges (unbiased sampling frame, see Gundersen, 1977) shown in Fig. 15 ensures the uniform sampling of particles if just the particles lying at least partly in the frame and not being intersected by the exclusion line are sampled. The frame can be rectangular or square. Note that many other (and often commonly used) sampling rules are not correct because they do not fulfill the above-mentioned condition (see Fig. 16 and Gundersen, 1977). Simple graphic demonstration of justification of arrangement of unbiased sampling frame is shown in Fig. 16B.

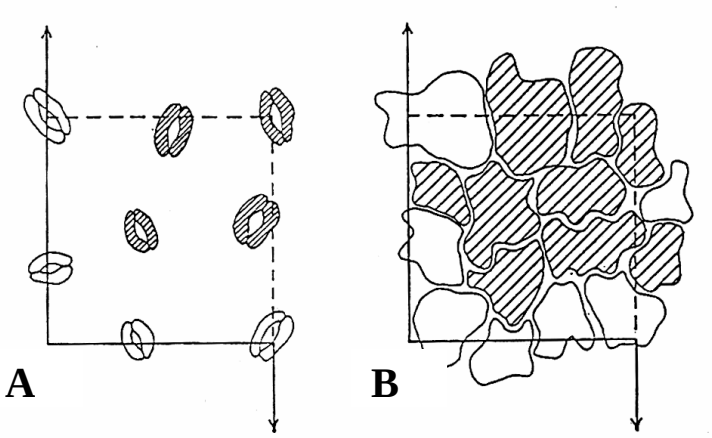

Fig.15: Unbiased sampling frame.

Rule: Sample just the particles that are lying at least partly in the frame and are not intersected by the (full-drawn) exclusion line. Four (hatched) stomata are sampled in A and nine ordinary epidermal cells in B.

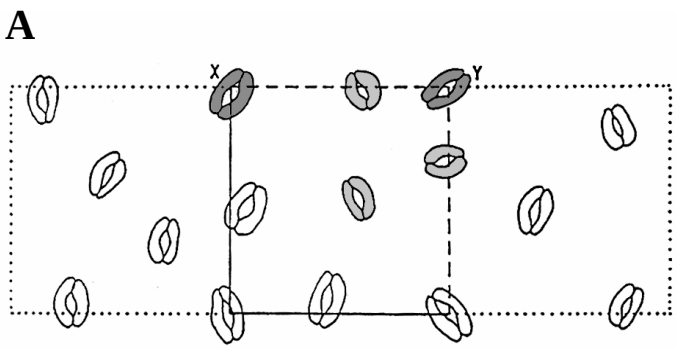

Fig. 16. Biased sampling rule.

A) Most commonly used biased criterion:

In addition to particles completely within the frame sample all particles intersected by the upper and right border and disregard all those intersected by the lower and left border, and sample any particle hit by the upper left corner and disregard those hit by the lower right corner. Following this rule, stoma X would be sampled by both the middle and left frame and stoma Y would be also sampled twice, by the middle and right frame.

B) Necessity of excluding line extensions.

If we do not apply the extensions of exclusion lines depicted in the unbiased sampling frame (Fig. 17), the curved particle showed in this picture would have been sampled twice. When making consistent net of sampling frames covering the whole area, the particle would be sampled by frame S and also by frame T.

1.4.2. Systematic uniform random sampling of segments

In order to get an unbiased result, the sampling frames should be moreover superimposed on the leaf surface uniformly (following, e.g. systematic uniform random sampling; for explanation see Fig.17).

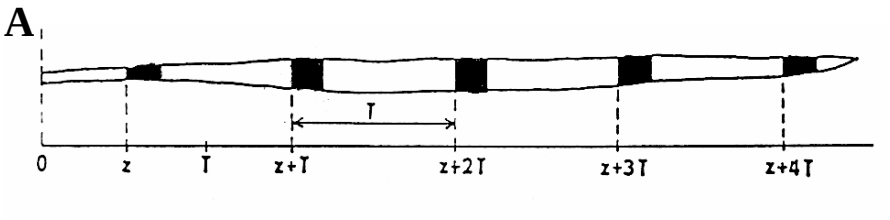

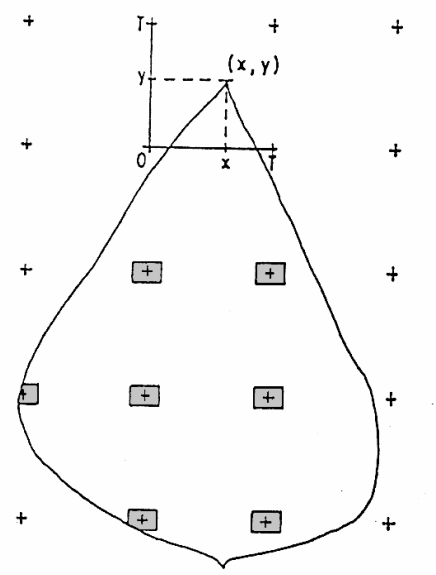

Fig.17. Systematic uniform sampling of leaf segments and sampling frames

A) Monocot monofacial leaf, e.g. that of grasses:
Firstly, the distance (T) (mm) between two consecutive segments is chosen. A random number (z) is then selected from the set {0,1,...,T-1}. The lower edges of the segments are placed in the positions z, z+T, z+2T, ... For example, if T=40mm, z=20mm, and the leaf length were 200mm, then the lower edges of segments would be cut at distances of 20mm, 60mm, 100mm, 140mm and 180mm from the leaf base. The sampling frames can be superimposed systematically in a band across the leaf in the middle of each segment.

B) Dicot bifacial leaf:
The distance (T) (mm) between the central points of the leaf segments is chosen first. Distances x and y are then selected at random from the set {0,1,...,T-1}. By placing the leaf tip in the position (x,y), the uniform random position of the leaf segments is ensured. The leaf segments are then cut as indicated in the figure. The sampling frames can be superimposed systematically in a band across the leaf in the middle of each segment.

1.4.3. Practical considerations: example of analysis of leaf epidermis

The above described unbiased sampling can be used for unbiased estimation of the numerical density or number of two-dimensional particles as well as for the unbiased estimation of their mean sizes (Kubínová, 1994): For example, the stomatal frequency ($n_A(stom)$) (mm^{-1}) on the lower (or upper) side of the leaf can be estimated by the formula:

$$est(n_A(stom)) = \frac{\sum_{j=1}^{m} n_j(stom)}{\sum_{j=1}^{m} a_j} \qquad (7)$$

where m is the number of sampling frames superimposed on the lower leaf surface, $n_j(stom)$ is the number of stomata sampled by the j-th frame (j=1,...,m), and a_j (mm^2) is the area of the intersection of the j-th frame with the leaf surface.

The area a_j (mm^2) can be easily estimated by point counting (see Weibel, 1979, and Section 1.2.2.). The point grid can be placed in the sampling frame (Fig. 18).

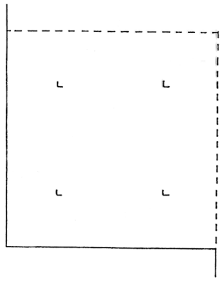

Fig. 18: Combination of an unbiased sampling frame and a point test system.
We choose the density of points according to the property of how much the studied structure is broken. Usually 4 points are enough, sometimes even 1 point is sufficient. We do not recommend to use more than 16 points in the frame if we use the ocular grid since the probability of error of observer is getting higher (making mistake during counting of hits).

The total number of stomata on the given side of the leaf can then be easily calculated by multiplying the corresponding stomatal frequency by the leaf area (which can be estimated by point counting again, see Kubínová, 1993, and Section 1.2.2.).

Analogously, the frequency and number of epidermal cells can be estimated.

The mean size of two-dimensional particles is estimated simply by the arithmetic mean of the sizes of the particles sampled by the frames. For example, when estimating the mean epidermal cell length ($\bar{l}(e.cell)$) (µm), cells are sampled by the unbiased sampling frames first, then their lengths ($l_i(e.cell)$, i=1,..., n) (µm) are measured and the following formula used:

$$est(\bar{l}(e.cell)) = \frac{1}{n} \cdot \sum_{i=1}^{n} l_i(e.cell) \qquad (8)$$

where n denotes the number of sampled epidermal cells.

Similarly, the mean stoma length or the mean width of ordinary grass epidermal cells can be estimated, as well as the mean cell area, the areas of cell replicas or projections being estimated, e.g. by point counting.

Using the unbiased sampling frames, also parameters of cell sections can be estimated, e.g. the number or mean area of profiles of cortex cells in a transverse root section.

1.5. Sampling in 2D

In order to obtain unbiased results in all above-mentioned methods, it is always necessary to follow some kind of random sampling; it is usually necessary to ensure that each item (e.g. position of a grid or a section) has the same probability to be sampled, i.e. to use the uniform random sampling. We have used such sampling procedures throughout the Chapter 1. The sampling procedures are summarized below.

1.5.1. Uniform random sampling of a point in 1D.

Sampling of a uniform random point from a line can be demonstrated by the example showing the sampling of a uniform random point along the axis of a carrot representing the uniform random position of its transverse section (see Fig. 19).

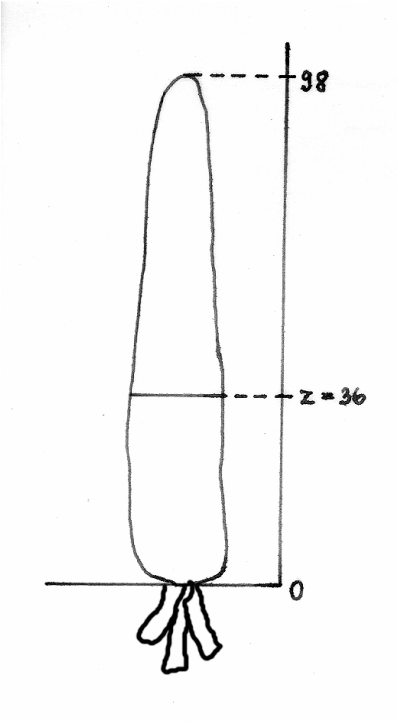

Fig. 19. Uniform random sampling of a point along the axis of a carrot.

The carrot in this figure is 98 mm long. Take a random number z from the set {0,1,2,...,97}. In this case it happened to be 36. Then z is the uniform random number determining a uniform random position of a transverse section cut from this carrot.

1.5.2. Systematic uniform random sampling of points in 1D.

Systematic uniform random sampling of points from a line can be demonstrated by the example showing the sampling of systematic uniform random points along the axis of a carrot representing the systematic uniform random positions of its transverse sections (see Fig. 20 and for sampling leaf segments see Fig.17A).

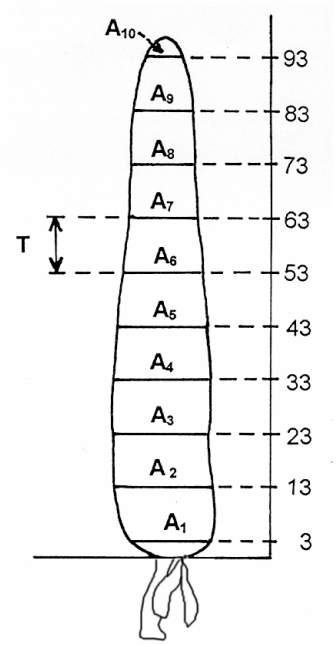

Fig. 20. Systematic uniform random sampling of points along the axis of a carrot.

Firstly, the distance T between two neighbouring points (lying on a line parallel to the carrot axis) is chosen (T=10 here). A random number is then selected from the set {0,1,2,...,T-1}. Here it happened to be 3. Therefore, the systematic uniform random points are given by the positions 3, 13, 23, ..., 93, which determine the systematic uniform random positions of transverse sections of the carrot to be cut at distances 3mm, 13mm, 23mm, ..., 93mm from the carrot base.

1.5.3. Uniform random sampling of a point in 2D.

Sampling of a uniform random point from a planar feature can be demonstrated by the example showing the sampling of a uniform random point from a flat leaf (see Fig. 21).

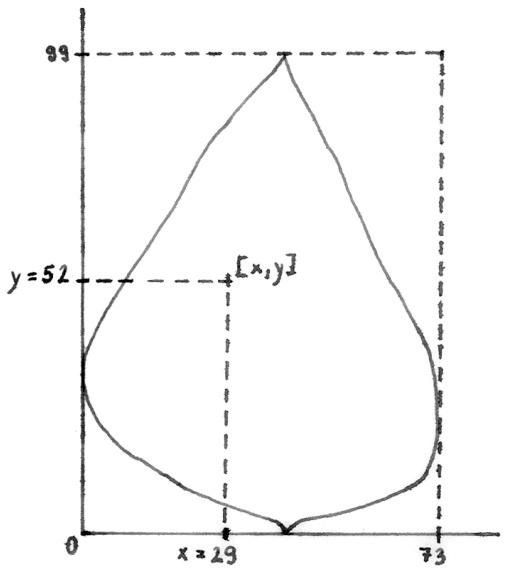

Fig. 21. Uniform random sampling of a point from a flat leaf.
The width of the leaf in this figure is 73 mm and its length is 99mm. Take a random number x from the set {0,1,2,...,72}and a random number y from the set {0,1,2,...,98}. In this case x happened to be 29 and y to be 52. Then the point [x,y] = [29,52] determines the uniform random position in a leaf, provided it is lying inside the leaf. (If it falls outside the leaf, another pair of random points x and y is taken and this procedure is repeated so long as the corresponding point is lying inside the leaf.)

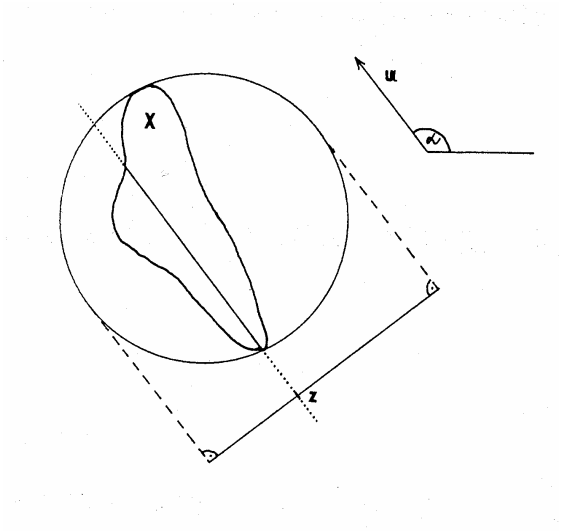

Fig. 22. Construction of an isotropic uniform random line in a planar feature X.
A circle circumscribing the feature X is constructed. Firstly, a uniform random angle α, $0 \leq \alpha < \pi$, is taken (it can be sampled as a random number from the set {0°, 10°,...,170°}). Secondly, a uniform random point z from the circle projection perpendicular to the direction given by the angle α is taken (which can be done by taking a random number from the set {0mm, 1mm, ...,57mm} in this case). Then the line going through the point z and parallel to the direction **u**, given by the angle α, is an isotropic uniform random line in a planar feature X, provided it is lying inside the X. (If it falls outside the feature X, the above procedure is repeated so long as the line is lying inside X.)

1.5.4. Systematic uniform random sampling of points in 2D.

Systematic uniform random sampling of points from a planar feature can be demonstrated by the example showing the systematic uniform random sampling of leaf segments from a flat leaf (see Fig. 17). The same principle was already explained in Section 1.2.3., Fig. 8., where the systematic uniform random sampling of test points superimposed on the flat leaf is described, which in fact corresponds to the uniform random positioning of the point grid on a leaf.

1.5.5. Isotropic uniform random orientation in 2D.

The construction of an isotropic uniform random line in a planar feature is shown in Fig. 22. If equidistant lines parallel to this line are added, we obtain a isotropic uniform random superposition of a linear test system on the planar feature.

1.5.6. Simple random sampling of 2-D particles.

Simple random sampling of planar particles is demonstrated in Fig.15 showing the unbiased sampling rule when counting stomata and ordinary epidermal cells.

2. MODULE II: Stereological methods

2.1. Introduction

Stereological methods are precise tools for the quantitative evaluation of the structure of 3-dimensional objects, based mainly on observations made on 2-dimensional sections or projections. For example, they can be used for the estimation of volume and surface of cells composing a tissue under study.

The term of stereology was coined in 1961 when the International Society for Stereology was founded. Its foundation was motivated by the need of researchers in material and life sciences to give rigorous theoretical basis to the solution of their 'stereological' problems with estimation of 3D characteristics of structures studied. The theory as well as applications of stereological methods to material and biomedical sciences are developing fast (for reviews see Weibel, 1979, Gundersen el al., 1988a,b, Cruz-Orive and Weibel, 1990, Howard and Reed, 1998). However, their applications in plant biology are still very rare.

In botanical research the early developed stereological methods were discussed in several surveys (Briarty, 1975, Parkhurst, 1982, Toth, 1982). Applications of some recently developed methods on plant material are described in Kubínová (1993, 1994, 1998). Some of the parameters, which can be estimated by stereological methods are listed below:

- **VOLUME** (leaf volume, root volume, volume of vascular tissues in a stem, etc.);
- **VOLUME DENSITY** (proportion of tissues in an organ, such as proportion of primary cortex in a root, proportion of epidermis in a leaf, proportion of intercellular spaces in mesophyll, etc.);
- **NUMBER** (number of mesophyll cells in a leaf, number of cortical cells in a root, etc.);
- **SURFACE AREA** (e.g. exposed surface area of mesophyll in a leaf);
- **LENGTH** (e.g. root length);
- **MEAN PARTICLE VOLUME** (mean cell volume, mean volume of nuclei, etc.);
- **MEAN PARTICLE SURFACE AREA** (e.g. mean mesophyll cell surface area).

In the past years the importance of proper sampling in stereology was realised, so that stereology is sometimes regarded as 'a sampling theory for populations exhibiting a geometrical structure'. From this point of view there are two basic approaches to stereological inference: a design-based and a model-based approach. In design-based stereology the studied object is regarded as non-random, deterministic and the stereological parameters are calculated with respect to the randomness assumed for the sampling; e.g., random sampling is achieved by the random positioning of a planar section. Under the model-based approach the randomness is assumed for the studied object or can be regarded as a realisation of a spatial stochastic process. Under the model-based approach the probe thus does not need to be random.

The design-based stereological methods will be treated throughout this textbook. In biological applications the design-based approach appears to be more appropriate because biological structures often cannot be treated as random. They are often ordered; they often exhibit some degree of anisotropy or non-homogeneity. And the design-based methods, as mentioned above, place practically no requirements on the shape and organisation of the studied structure. Moreover, these methods lead to unbiased or at least practically unbiased estimates of stereological parameters.

In following sections practical considerations will be demonstrated on two types of objects: more or less anisotropic monocot grass leaf and isotropic dicot bifacial leaf.

2.2. Sampling

The correct application of design-based stereological methods is critically dependent on proper sampling - sampling of tissue blocks, sections, test frames, point grids, etc. In stereology, geometrical properties of the object (e.g., the leaf) are derived from the information collected from relatively small parts of the object (e.g., leaf sections). That means, when evaluating a specific average parameter of the object (e.g., the proportion of mesophyll in the leaf or the number of mesophyll cells in a leaf), just its specific parts (e.g., leaf sections) are measured to estimate the parameter. In order to get sensible results, these parts should be sampled in a way ensuring the estimate to be close enough to the true value of the parameter and yielding no systematic bias (i.e., the estimate should be unbiased, see Cochran, 1977). This can be achieved by proper sampling.

For example, the proportion of mesophyll in the leaf can be estimated by the proportion of mesophyll in the leaf sections without bias if these sections are sampled along the leaf uniformly (see Section 2.3., Fig. 23). Examining sections of only one specific part of the leaf (e.g., only in its middle part) causes biased results when estimating the average values for the whole organ unless the mesophyll is distributed homogeneously in the leaf. This is not very likely to occur in most cases, taking into account the developmental as well as biochemical and physiological gradients taking place in leaf lamina. It means that every leaf section (of specified orientation) must be equally likely to be sampled for the measurement. Otherwise the results can differ from the reality dramatically.

Similarly, the proper sampling must be followed when estimating a mean size of specific particles in some structure, e.g. the mean volume of mesophyll cells in a leaf. The true value of this parameter is clearly given by the sum of volumes of all mesophyll cells in the leaf divided by their number. When estimating this parameter we can sample only some of the cells and measure their volume. It is clear that the estimate is unbiased just if the process of cell sampling guarantees every mesophyll cell in the leaf to be sampled for the measurement with equal probability. Picking up the cells, e.g. just from the central part of the leaf, clearly does not fulfil this requirement, the cells from other than central parts having no chance of being sampled. This kind of sampling could be justified only if the cell volumes did not vary along the leaf. There is some evidence that this is not true in general (for barley (*Hordeum vulgare* L.) leaves see Kubínová, 1989, for the gradient of the mean area of transverse sections of mesophyll cells in Arabidopsis thaliana leaves see Pyke, Marrison and Leech, 1991, for the gradient of stomatal frequency in various types of leaves see Slavík, 1963, Pazourek, 1966).

Proper sampling for individual measurement procedures is described in the following sections where selected stereological methods are presented.

2.3. Volume density: systematic sampling for point-counting method

The principle of the point-counting method (Weibel, 1979) applied to area estimation was already described in Section 1.2.2. This method can also be used for the estimation of the volume density (or proportion) of a component in an object (if we apply systematic uniform random sampling), e.g. the volume density of mesophyll in the leaf ($V_V(mes)$) which is defined by the ratio of the volume of mesophyll ($V(mes)$) (mm^3) to the leaf volume ($V(leaf)$) (mm^3):

$$V_V(mes) = \frac{V(mes)}{V(leaf)} \qquad (9)$$

Procedures leading to a practically unbiased estimate of $V_V(mes)$ are described below. To discuss practical considerations of method applications, two types of approaches are demonstrated on monocot monofacial grass leaf and dicot bifacial leaf, which differ in their shape.

2.3.1. Application on monocot grass leaf

In relatively narrow leaves, such as grass leaves, just a few transverse sections (i.e. sections perpendicular to the longitudinal axis of the leaf) are cut systematically with a random position of the first section (so called systematic uniform random sampling; for explanation see Fig.17). A point grid is superimposed on the sections (see Fig.23) and points which hit mesophyll as well as points hitting the leaf sections are counted. The proportion of mesophyll in the leaf is then estimated by the ratio of these two point counts:

$$estV_V(mes) = \frac{\sum_{j=1}^{n} P_j(mes)}{\sum_{j=1}^{n} P_j(leaf)} \qquad (10)$$

where n is the number of examined sections, $P_j(mes)$ (j=1,...,n) is the number of test points hitting mesophyll in the j-th section, and $P_j(leaf)$ (j=1,...,n) is the number of test points which hit the j-th leaf section.

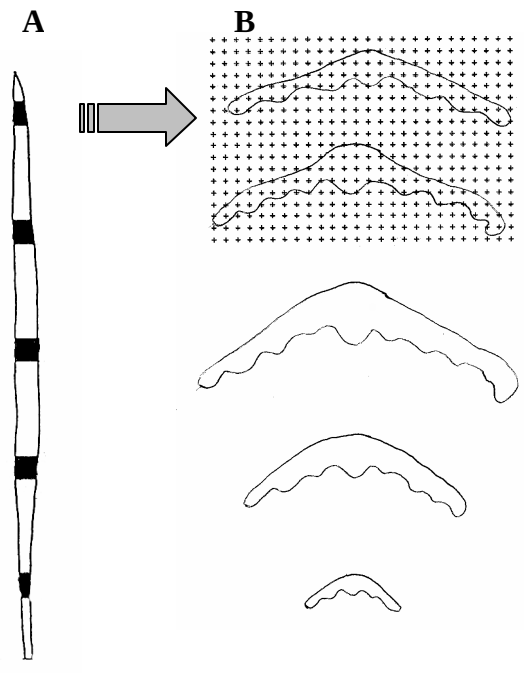

Fig. 23: Principle of systematic uniform random sampling when estimating volume density

A) sampling of leaf segments (in detail explained in Fig. 17A)

B) Cross sections made from sampled segments

C) Point grid superimposed on the transverse section of the barley leaf. Points hit different leaf tissues (epidermis, mesophyll cells, intercellular spaces, vascular tissue).
(a) = area unit corresponding to one test point of the grid, the length of one square side is 50 μm here.
(a = 50x50 μm^2 = 0.0025 mm^2, P(mes) = 8 and P(leaf) = 15 here.)

The procedure shown in Fig.17 ensures that every position of the transverse section has the same probability of being sampled for the measurement. If only several fixed positions (e.g., 1cm from the leaf base, in the middle of the leaf and 1cm from the tip) were chosen, the other positions would be disregarded which would lead to a biased estimate (see also section 2.2.).

The distance (*T*) between sections is chosen for each group of leaves (e.g., for leaves of a certain variant) separately. It is given by the ratio of the mean length of the leaves to the average number of sections to be examined per leaf (five sections per leaf can be sufficient - see section 3.).

2.3.2. Application on dicot bifacial leaf

In broad flat leaves the proportion of mesophyll can be estimated from leaf segments, again cut systematically from the leaf, by the procedure indicated in Fig.17B. One central section per segment is then examined and formula (10) used.

Analogously, the volume density of intercellular spaces, epidermis and other tissues in the leaf can be estimated, as well as the proportion of different tissue types in a root or in a stem. The same procedures can be used also for the estimation of the proportion of intercellular spaces in the mesophyll - here we obviously count points hitting intercellular spaces in all examined sections and divide this number by the number of test points which hit the mesophyll.

The point grid should be superimposed on the section uniformly at random, e.g., by defining a fixed reference point in the section (it can be, e.g., the intersection point of left and upper edges of the section) and placing the grid uniformly at random with respect to this point (following the procedure shown in Fig. 8A where the reference point of the leaf is represented by the leaf tip). The grid of central points of the leaf segments does not need to be squared. In oblong leaves a rectangular grid can be more appropriate. The distance between points of the grid is chosen in dependence on the average number of segments to be examined per leaf (see section 3.).

2.4. Cavalieri's estimator

Cavalieri's principle (Gundersen & Jensen, 1987, Michel & Cruz-Orive, 1988) is a method of estimating volume, based on cutting the object with systematic parallel planes a known distance (*T*) apart. The volume of the object is then estimated by the sum of the section areas multiplied by *T*. Usually, it is convenient to estimate the section areas by point counting.

Cavalieri's principle can be used for the estimation of the volume of a grass leaf or generally narrow leaf, which can be totally cross-sectioned (Fig.24) : Firstly, the systematic transverse sections are sampled as described in Fig.17. They can be identical with the sections used for the estimation of V_V (*mes*) (see Fig.23B). A point grid is superimposed on the sections (Fig. 23C) and the leaf volume ($V(leaf)$) (mm^3) is estimated by the sum of areas of the leaf sections (Fig.24) estimated by the point-counting method and multiplied by the distance between two consecutive sections (*T*) (mm):

$$estV(leaf) = T \cdot a \cdot \sum_{j=1}^{n} P_j(leaf)$$

(11)where *n* is the number of examined sections, *a* (mm^2) is the area unit corresponding to one test point of the point grid (see Fig. 23) and $P_j(leaf)$ (j=1, ...,n) is the number of test points hitting the j-th leaf section.

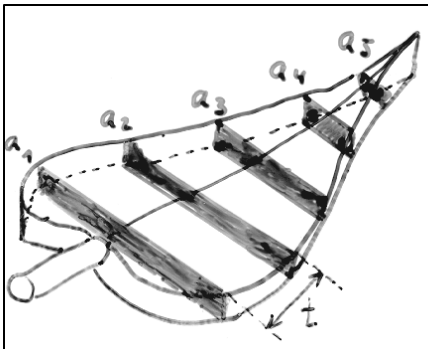

Fig. 24: Estimation of leaf volume of a narrow leaf by Cavalieri estimator.
T - systematic distance between cross sections
a_1,..,a_5 - areas of cross sections identified by point-counting method, then leaf volume V_l estimated by the formula 11 is here:
est V_l = T . ($a_1 + a_2 + a_3 + a_4 + a_5$)

Cavalieri's principle can also be used for the estimation of the volume of other plant organs, or the volume of a given type of tissue present in a plant organ, e.g. the volume of mesophyll in a leaf (see Fig. 23C) or the volume of cortex in a root.

2.5. Disector

The unbiased counting or sampling of three-dimensional particles (e.g. mesophyll cells) can be achieved by using a stereological principle of disector (Sterio, 1984, Gundersen, 1986, Kubínová, 1994). It should be noted that estimating the cell number by counting cell profiles in tissue sections is not correct because higher cells are more likely to be hit by the section than smaller ones, i.e. the number of cell profiles depends on the height of cells normal to the plane of sectioning.

Disector is a three-dimensional probe which samples three-dimensional particles with a uniform probability in three-dimensional space, irrespective of their size and shape (Fig.25). The disector is delimited by two parallel planes and it in fact aims at sampling top points of particles lying in between. In principle one simply counts particles that are hit by only one of the planes of the disector but not by the other (i.e. particles seen in one section and not seen in the other one are counted). It is clear that the following General Requirement must be fulfilled (Sterio, 1984): Any particle profile from the set of particle profiles should be unambiguously identifiable as belonging to the same particle (Fig. 26).

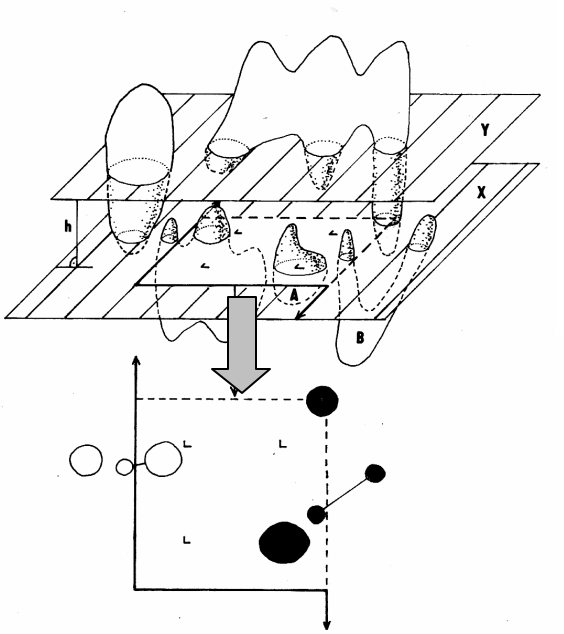

Fig. 25: The disector principle.
Sample just the particles with profile sets sampled by the unbiased sampling frame in the lower plane which are not intersected by the upper, look-up plane. Particles A and B are sampled by the disector here.

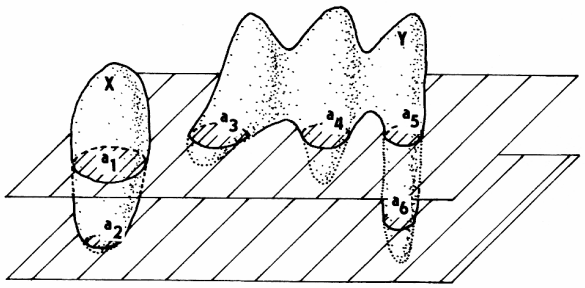

Fig. 26: General Requirement for the disector.
Any particle profile from the set of particle profiles should be unambiguously identifiable as belonging to the same particle. In the situation shown here we must be able to recognize that profiles a_1 and a_2 belong to the particle X while profiles a_3, a_4, a_5, and a_6 belong to the particle Y.

In practice, when using the disector principle, e.g. for the estimation of the number of mesophyll cells in the leaf, corresponding places in two parallel planes are observed (Fig.25 and Fig.27). At first, in one of the planes sets of cell profiles (including the straight lines connecting the profiles, see Fig. 25) are sampled by an unbiased sampling frame (Fig.15). Disector selects all cells with profile sets being sampled by the frame, which are not intersected by the second, look-up plane.

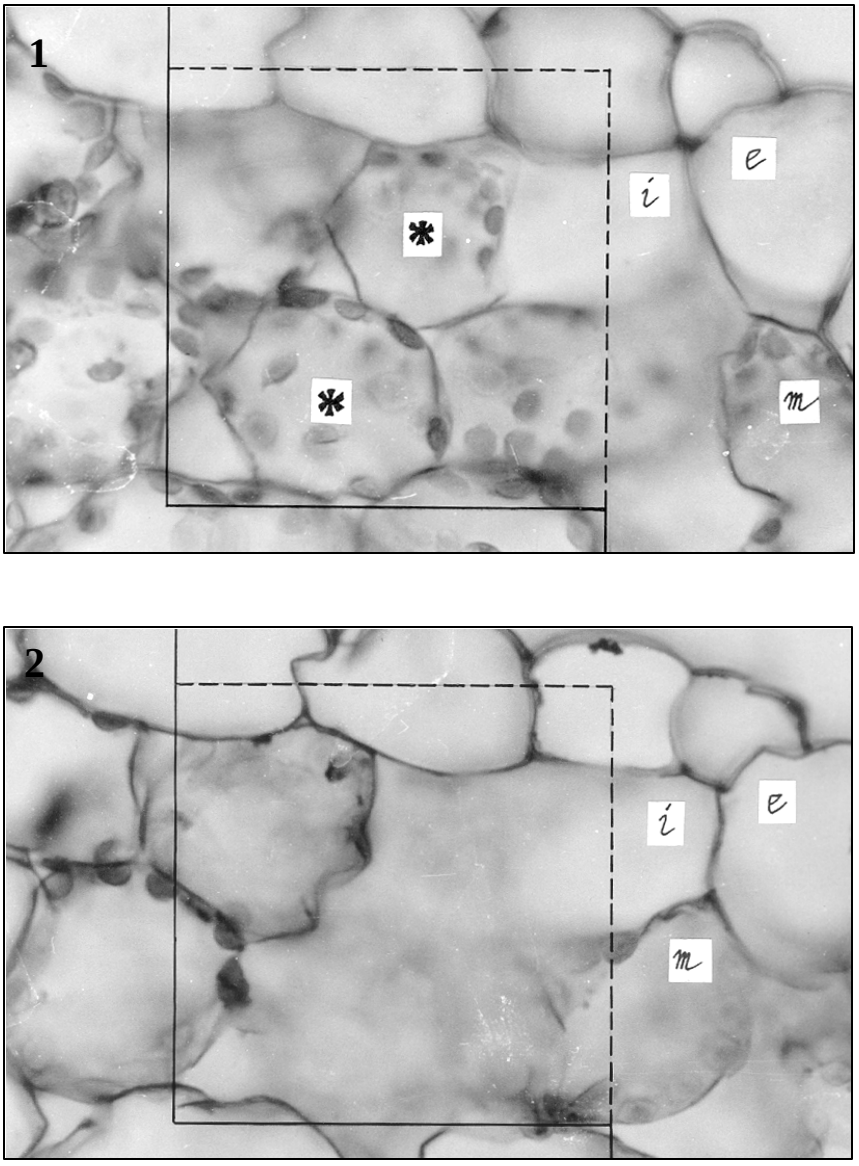

Fig.27. Optical disector in a transverse section of barley leaf. Two different planes of focus represent the disector planes. Disector counts the cells fulfilling the following conditions at the same time:

1) In the first disector plane, the cell section is sampled by the unbia-sed sampling frame (Fig.15). 3 Perticles are selected here and two of them marked by * are those which are later selected by disec-tor as implies from the 2).
2) The cells marked by * in 1) do not intersect the second, look-up disector plane, thus they are sampled by the disector with the first plane 1) shown above. disector thus samples two cells here.

m = mesophyll cell;
i = intercellular spaces;
e = epidermal cell.
(from Albrechtová and Kubínová 1991)

The disector planes are represented either by two distinct "physical" sections which are compared (physical disector) or by two thin optical sections inside one thick physical section when the particles are counted during focussing through this thick section (optical disector, see Gundersen, 1986).

If the position of the disectors is uniform over all possible positions in the leaf and a point grid of p points is placed in the counting frame, the number of mesophyll cells ($N(m.cell)$) can be estimated by a practically unbiased estimator:

$$estN(m.cell) = \frac{\sum_{i=1}^{n} Q_i^-(m.cell)}{\sum_{i=1}^{n} P_i(leaf)} \cdot \frac{p}{a' \cdot h} \cdot V(leaf) \qquad (12)$$

where n is the number of disectors, $Q_i^-(m.cell)$ (i=1,...,n) is the number of mesophyll cells sampled by the i-th disector, $P_i(leaf)$ (i=1,...,n) is the number of points of the p-point grid in the i-th frame hitting the leaf section, a' (μm^2) is the (actual) area of the frame, h (μm) denotes the distance between the disector planes (disector height) and $V(leaf)$ (μm^3) is the leaf volume (Fig. 25).

In formula (12) the combination with the point-counting method is used. For the estimation of the leaf volume ($V(leaf)$) in grass leaves see the previous section 2.4. In flat bifacial leaves the leaf volume can be calculated by the product of the leaf area and the mean leaf thickness (for details see Kubínová, 1993).

Using the disector principle, the mean particle volume, e.g. the mean mesophyll cell volume in the leaf ($\bar{v}(m.cell)$) (μm^3), can also be estimated (Gundersen, 1986):

$$est(\bar{v}(m.cell)) = \frac{\sum_{i=1}^{n} P_i(m.cell)}{\sum_{i=1}^{n} Q_i^-(m.cell)} \cdot \frac{a' \cdot h}{p} \qquad (13)$$

where $P_i(m.cell)$ (i=1,...,n) is the number of points of the p-point grid in the i-th frame hitting the mesophyll cell profiles, n is the number of disectors, $Q_i^-(m.cell)$(i=1,...,n) is the number of mesophyll cells sampled by the i-th disector, a' (μm^2) is the (actual) area of the frame, and h (μm) denotes the distance between the disector planes (disector height) (Fig. 25).

The procedures for the estimation of the number and/or the mean mesophyll cell volume in two leaf types are proposed below.

2.5.1. Application on monocot grass leaf

In relatively narrow leaves, such as grass leaves, just a few leaf segments are cut systematically with a random position of the first one (so called systematic uniform random sampling Section 1.5.2.; for explanation see Fig.17). One transverse section (cut from the lower edge of the segment, see Fig. 23) per segment is then examined. The disector counting frames are then placed in the lower disector plane (i.e. in the optical (Fig. 27) or physical section of the leaf) uniformly at random, e.g. by defining a fixed reference point in the section (such as one of the corners of the cover glass or the uppermost point of the main leaf ridge in the section; see Fig. 8) and placing the frames systematically and uniformly at random with respect to this point (Fig. 28). Then the mesophyll cells and points hitting the leaf section and/or cell profiles are counted over all disectors in all sampled sections and formulas (12) and/or (13) are used.

The distances (T), (d_1), (d_2) are chosen for each experimental group of leaves separately, depending on the average number of segments and disectors to be examined per leaf (see Section 3.).

The above described procedure was used for the estimation of the number and mean volume of mesophyll cells in barley leaf (Albrechtová & Kubínová, 1991, Kubínová, 1991).

Analogous procedure, though possibly with practical limitations, can be used for counting and measuring cells in any oblong plant organ, such as a root or a stem.

If it is not possible to fix and embed leaf segments which are entire width of the leaf, the procedure for bifacial leaves described below can be recommended.

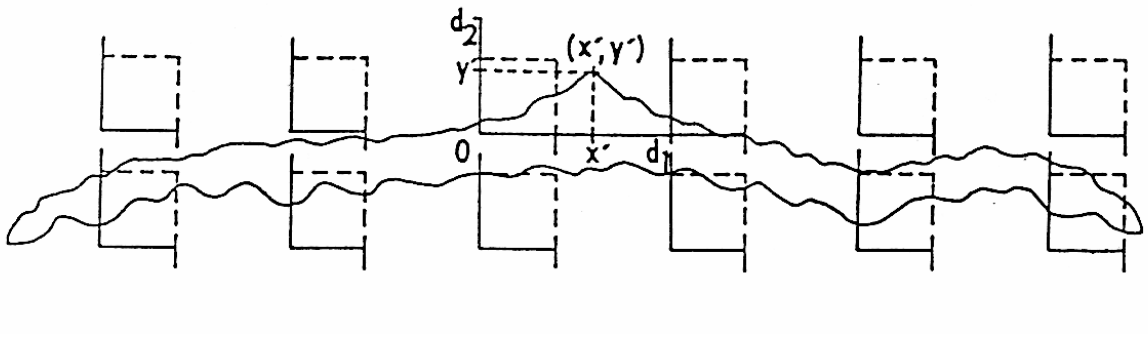

Fig. 28: Systematic uniform random position of the disector sampling frames.
The distances (d_1), (d_2) (μm) between the neighbouring frames are chosen first. Numbers x and y are then selected at random from the set {0,1,...,9}. By placing the system of frames on the leaf section so that the uppermost point of the main ridge lies in the position (x',y') ($x'=d_1.x/10$, $y'=d_2.y/10$) the uniform random position of the system of sampling frames is ensured.

2.5.2. Application on dicot bifacial leaf

In broad flat leaves several leaf segments should be cut systematically from the leaf, by the procedure indicated in Fig.17B. One central section per segment is then examined, the disector counting frames being positioned in the lower disector plane uniformly at random again (here the reference point might be the intersection point of left and upper edges of the section). The number of mesophyll cells in the leaf can be then estimated by formula (12) and the mean cell volume in the leaf by formula (13).

The grid of central points of the leaf segments (Fig.17B) need not be square. In oblong leaves a rectangular grid can be more appropriate. The distance (*T*) is again chosen depending on the average number of segments to be examined per leaf.

2.6. Estimation of surface area.

2.6.1. Review of methods

The stereological estimation of the surface area of a structure (e.g. exposed surface area of mesophyll in the leaf) is based either on counting intersection points between the structure surface and line probes or on the measurement of the length of the intersection between the surface and test planes going through the structure. The orientation of test lines or test planes can be arbitrary only if the structure has the same geometrical properties in all directions of space, i.e. if it is isotropic.

Otherwise isotropic random orientation of test lines or test planes is required. It means that every orientation must have the same probability to be chosen for the measurement. Most frequently used stereological methods for the unbiased estimation of surface area suitable for practical application are the method of vertical sections ensuring the isotropic orientation of test lines and the orientator method ensuring the isotropic orientation of test planes. Recently, the highly efficient methods based on using spatial grids of test lines (Sandau, 1987, Cruz-Orive and Howard, 1995, Kubínová and Janácek, 1998) have emerged.

2.6.1. Method of vertical sections

The method of vertical sections (Baddeley et al., 1986) is very suitable for evaluation of anisotropic structures, e.g. for estimating the exposed surface area of mesophyll in the leaf (S(exp)) (mm^2) (i.e. the surface area of mesophyll cell walls exposed to intercellular spaces).

The area of the exposed surface of mesophyll is proportional to the mean number of intersection points between this surface and a straight line probe placed uniformly and isotropically at random in space. The vertical sections method enables such position and orientation of line probes. Vertical sections are plane sections longitudinal to a fixed (but arbitrary) axial direction, or perpendicular to a given horizontal plane (Fig. 29A).

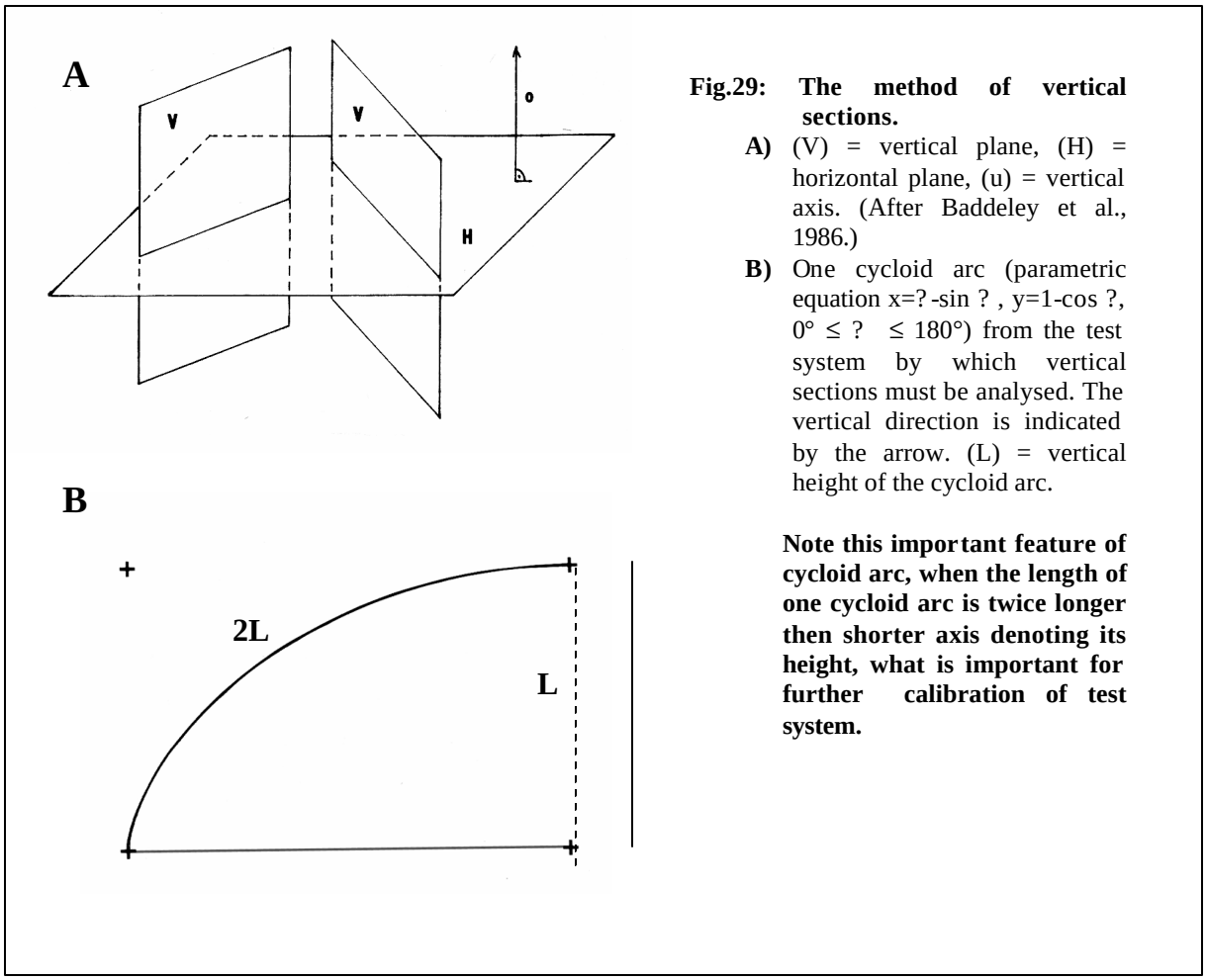

Fig.29: The method of vertical sections.

A) (V) = vertical plane, (H) = horizontal plane, (u) = vertical axis. (After Baddeley et al., 1986.)

B) One cycloid arc (parametric equation x=? -sin ? , y=1-cos ?, 0° ≤ ? ≤ 180°) from the test system by which vertical sections must be analysed. The vertical direction is indicated by the arrow. (L) = vertical height of the cycloid arc.

Note this important feature of cycloid arc, when the length of one cycloid arc is twice longer then shorter axis denoting its height, what is important for further calibration of test system.

In practice, vertical sections are cut first and test lines are superimposed on the sections. The uniform position and isotropic orientation of test lines are guaranteed by the following procedure:

1. Vertical sections are sampled so that they intersect the horizontal plane in isotropic uniform random straight lines (for practical construction see Fig. 30, 31).

Fig. 30: Construction of vertical sections of the grass leaf

Firstly, the systematic uniform random sampling of leaf segments is done as shown on the left (see also Fig.17A). In the horizontal plane of the first segment (i.e. the nearest one to the leaf base), angle a_1 ($0° = a_1 < 180°$) is selected uniformly at random (e.g., a_1 is a random number from the set {0°, 10°, 20°,...,170°}). The vertical sections of the first segment are cut in this orientation. With m segments in the leaf, the orientation of vertical sections in the j-th segment is given by the angle $a_j = a_1 + (j-1) \times (180°/m)$ (j=1,...,m).

For example, if m=5 and a_1=10°, then a_2=10° + 1 x (180°/5) = 46°, a_3 = 82°, a_4=118°, and a_5=154°.

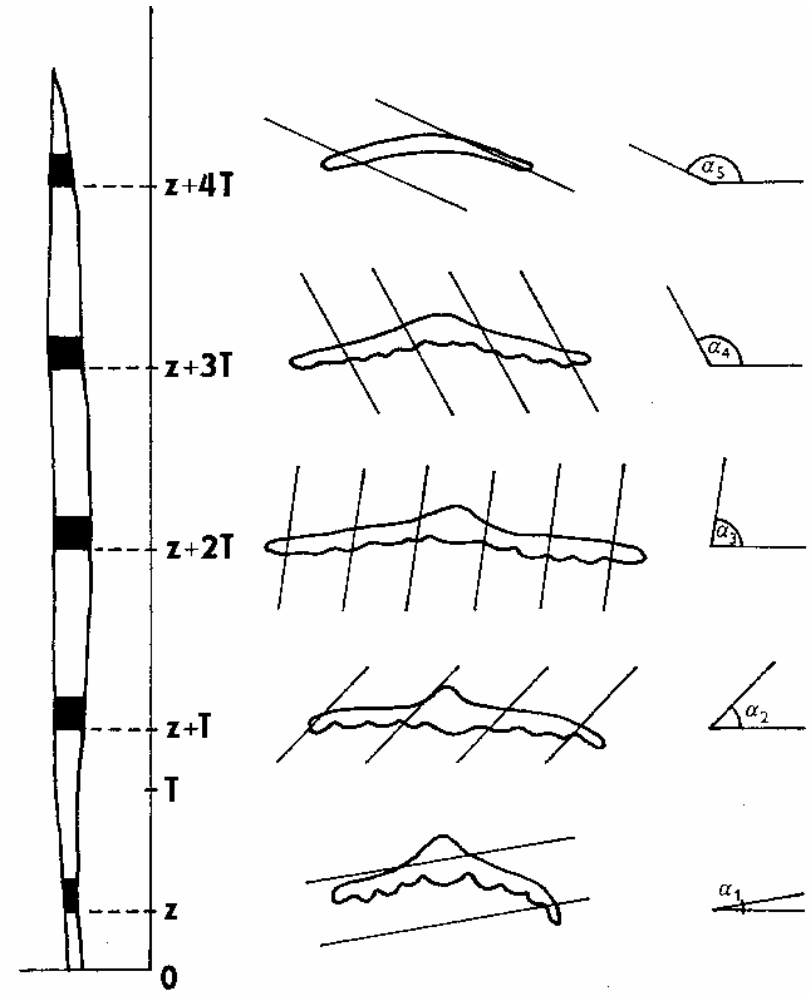

Within the segment, the series of equidistant parallel sections (in the figure illustrated by lines intersecting the sampled segments seen from above) are cut in a way analogous to the one described in Fig.17A. The equal distance between the vertical sections can also be achieved by cutting serial sections of the segment and taking every k-th section for the measurement (number k is chosen in dependence on the desired distance between the sections), beginning with the i-th section (i is a random number from the set {1, 2,...,k}).

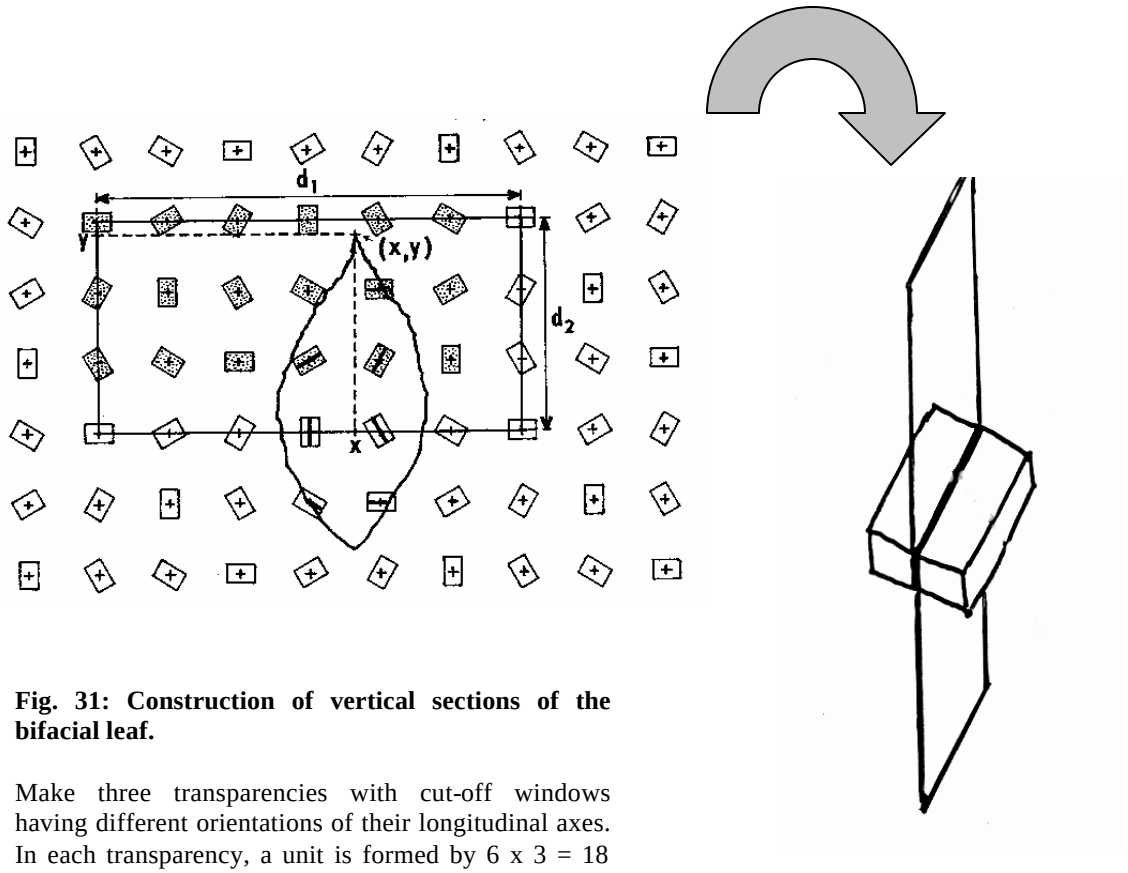

Fig. 31: Construction of vertical sections of the bifacial leaf.

Make three transparencies with cut-off windows having different orientations of their longitudinal axes. In each transparency, a unit is formed by 6 x 3 = 18 windows (dotted windows in the upper figure). The orientations of the windows in the first row of the unit are given subsequently by six angles d + m.30° (m=0,1,...,5) and the orientations of windows in the first column by three angles d + n.60° (n=0,1,2). Take d = 0° for the first transparency, d = 10° for the second, and d = 20° for the third one (i.e., in the first transparency the first row of the corresponding unit is formed by windows with orientations given by 0°, 30°, 60°, 90°, 120°, 150° and the orientations of the windows of the first column are given by angles 0°, 60°, 120° - see the upper figure). Now select a random number z from the set {0, 1, 2}. If z=0 then use the first transparency, if z=1, use the second one and if z=2 use the third one. Make a rectangle by connecting the central points of seven windows neighbouring in a row and the central points of four windows neighbouring in a column (see the upper figure). This rectangle represents the area unit corresponding to the unit of windows. Superimpose the transparency so that the leaf tip coincides with a uniform random point of this rectangle (i.e., with point (x,y), where x is a random number from the set $\{0,1,...,d_1-1\}$ and y is a random number from $\{0,1,...d_2-1$; d_1 is the width (mm) of the rectangle and d_2 is its height (mm)). The leaf segments to be cut are now determined by the windows of the transparency. One central section of each segment is then examined (See fig. 32 and 33).

2. A special test line system made of cycloid arcs (see Fig.29B, 32, 33) combined with a point grid, is superimposed on each examined vertical section and the intersection points between exposed surface of mesophyll and test lines ($I_j(exp)$, j=1,...,n), as well as points hitting the leaf section ($P_j(leaf)$, j=1,..., n) are counted. The vertical axis should be identifiable on each vertical section, and the vertical height of the cycloid arcs should be parallel to that axis (Fig.29B, 32, 33). Then the exposed surface area of mesophyll in the leaf ($S(exp)$) (mm^2) can be estimated by the formula:

$$est(S(\exp)) = 2 \cdot \frac{p}{l} \cdot \frac{\sum_{j=1}^{n} I_j(\exp)}{\sum_{j=1}^{n} P_j(leaf)} \cdot V(leaf) \qquad (14)$$

where n is the number of examined vertical sections, p/l (mm^{-1}) is the ratio of test point number to cycloid arc (actual) length (the length of a cycloid arc equals twice its height, see Fig. 29B), and $V(leaf)$ (mm^3) is the leaf volume (see section 2.4.).

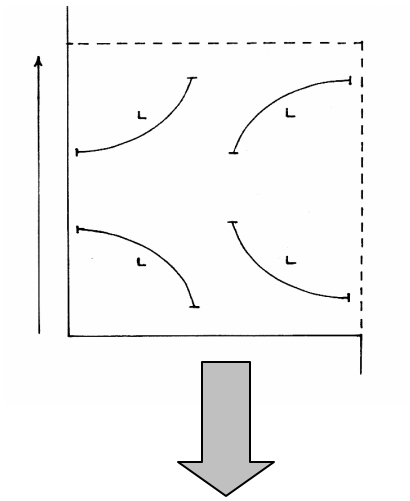

Fig. 32: Example of a cycloid test system combined with a point grid.

The vertical direction is indicated by the arrow. Such combination of test systems is necessary to use when estimating parameter of surface area from sampled sections not the whole object.

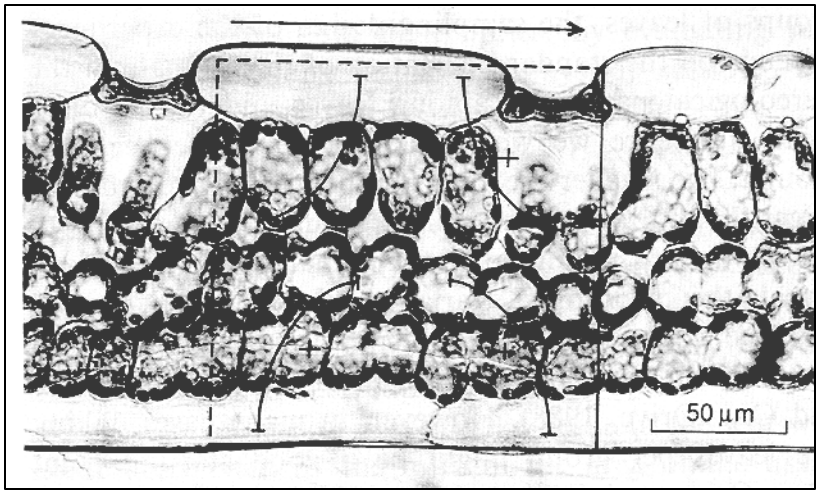

Fig. 33. Cycloid test system superimposed on the vertical section of the barley leaf.

The vertical direction is indicated by the arrow. When using the formula 14 for determining inner leaf surface, i.e. surface of mesophyll cell walls neighbouring with intercellular spaces used for gas exchange in the leaf, here: p/l = 1/72 μm^{-1} = 1.4 x 10^{-5} mm^{-1}, I(exp) = 4, and P(leaf) = 4

2.6.1.1. Application on a monocot grass leaf

In a grass leaf, the vertical axis can be represented by the longitudinal axis of the leaf and so the vertical sections are sections parallel to the leaf axis, i.e. perpendicular to the transverse sections of the leaf (the procedure is shown in detail in Fig.30). A cycloidal test system is then superimposed on the sections and formula (14) used. (The orientation of the vertical axis being identical with the orientation of longitudinal axes of epidermal cells seen in the section, the test system can be set up in the right orientation, i.e. so that the vertical height of cycloid arcs is parallel to the vertical axis - see Fig. 33).

The visibility of the leaf segment as seen from the horizontal plane (needed for the proper orientation of vertical sections) can be achieved by staining the segment during embedding and by cutting a few transverse sections first.

If it is not possible to fix and embed leaf segments which are the entire width of the leaf, an analogous, yet more laborious procedure with smaller leaf segments sampled across the leaf width can be used.

2.6.1.2. Application on a dicot bifacial leaf.

In leaves, which can be flattened on a plane, this plane can represent the horizontal plane, i.e. the vertical sections are sections perpendicular to the leaf surface (with random orientation in the base plane - one possible way of their construction is shown in Fig. 31). A cycloidal test system is then superimposed on the sections and formula (14) used. (The vertical axis being perpendicular to the leaf surface, which can be seen in the sections, the test system can be set up properly, i.e., with the vertical height of its cycloid arcs parallel to the vertical axis). The vertical sections can also be used for the estimation of the exposed surface area of palisade and spongy mesophyll separately, if these two layers can be distinguished on transverse sections. Formula (14) can be used here, counting the intersection points between test lines and exposed walls of palisade or spongy mesophyll cells, respectively. By counting intersection points between test lines and overall surface of mesophyll cell walls the surface area of all mesophyll cells in the leaf can be estimated.

In Fig.31 just one of the many possible ways of the construction of vertical sections is shown. Other units of oriented windows can be used (e.g., unit of 4 x 4 = 16 windows with the orientations given by 0°, 45°, 90° and 135° in the first row and the first column).

2.6.2. Orientator

2.6.2.1. Generation of isotropic uniform random sections using orientator

The method of orientator (Mattfeldt et al., 1990) enables to generate isotropic uniform random (IUR) sections (i.e. it enables such sampling of orientations of test planes that every orientation has the same probability to be sampled) of the object under study in practice. The subsequent evaluation of these sections can lead to the unbiased estimate of the surface area of a given structure. This method has the same mathematical background as that used for generating IUR linear probes on vertical sections (Section 2.6.1. and Baddeley et al., 1986). For the illustration of the orientator principle, its simplest (in our opinion) version published by Howard and Reed (1998, Fig. 34) will be presented:

(1) A uniform random slab of the object (see Fig. 17A) is removed and a vertical direction defined for that slab. This direction must be identifiable and is fixed for the remainder of the sectioning

process. In the example shown in Fig. 34A, the vertical direction has been marked on the side of the carrot and is parallel to its long axis.

(2) The slab is placed with uniform random position and arbitrary rotation on a uniformly divided Φ clock with the original vertical axis of the slab normal to the plane of the clock. A uniform random number between 0 and 9 is generated using a random number table. In the example 7 has been selected. The slab is then cut perpendicular to the plane of the clock and along the random direction selected (i.e. 7-7).

(3) One of the two pieces of the slab that has been generated by step 2 is chosen at random. The newly generated flat face of this piece is then placed with uniform random position, face down on the cosine-weighted Θ clock, with the original vertical axis of the piece along the 0-0 line of the clock. Finally a second uniform random number between 0 and 9 is generated using a random number table. In the example 3 has been selected. The piece is then cut perpendicular to the plane of the clock and along the random direction selected (i.e. 3-3). This final cut face is an isotropic uniform random plane section through the original object.

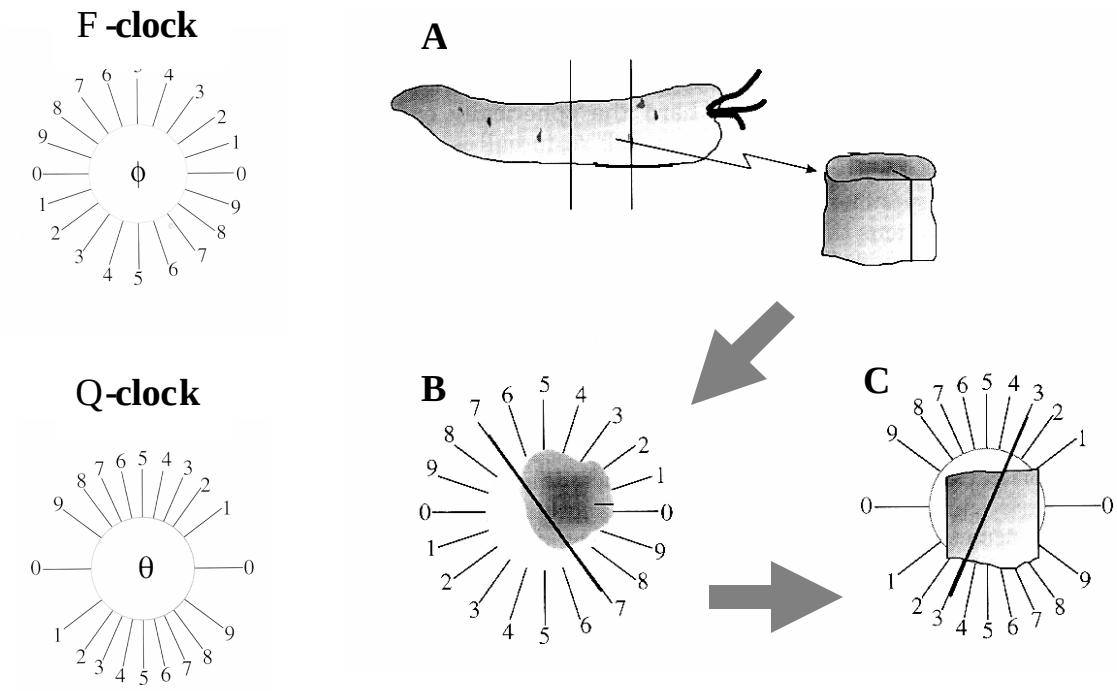

Fig. 34: Principle of orientator for generation of isotropic uniform random (IUR) sections: illustration on carrot (From Howard and Reed, 1998).

A) A uniform random slab of the object is removed and a vertical direction defined for that slab. This direction must be identifiable and is fixed for the remainder of the sectioning process. In the example the vertical direction has been marked on the side of the carrot and is parallel to its long axis.

B) The slab is placed with uniform random position and arbitrary rotation on a uniformly divided Φ clock with the original vertical axis of the slab normal to the plane of the clock. A uniform random number between 0 and 9 is generated using a random number table (i.e. 7 has been selected). The slab is then cut perpendicular to the plane of the clock and along the random direction selected (i.e. 7-7).

C) One of the two pieces of the slab that has just been generated is chosen at random. The newly generated flat face of this piece is then placed with uniform random position, face down on the cosine-weighted Θ clock, with the original vertical axis of the piece along the 0-0 line of the clock. Finally a second uniform random number between 0 and 9 is generated using a random number table (i.e. 3). The piece is then cut perpendicular to the plane of the clock and along the random direction selected (i.e. 3-3). This final cut face is an IUR plane section through the original object.

2.6.2.2. Estimation of surface area using orientator

The above mentioned procedure enables to construct isotropic uniform random sections of the object which can be used for the estimation of the surface area of its internal structure under study ($S(str)$) using the formula:

$$est(S(str)) = \frac{4}{p} \cdot \frac{\sum_{j=1}^{n} B_j(str)}{\sum_{j=1}^{n} A_j(obj)} \cdot V(obj) \qquad (16)$$

where n is the number of examined sections generated by the orientator, $B_j(str)$ (j=1,...,n) is the length of the intersection between the structure surface and the j-th section, $A_j(obj)$ is the area of j-th section of the object and $V(obj)$ (mm^3) is the object volume (see section 2.4.). This can seem to be difficult to be determined. But it is necessary to realize that the ratio $B_j(str)/ A_j(obj)$ is in fact the parameter, which we know to identify from the section 1.3.2.1., formula 5: B_A is the length of profiles of internal structure with the j-th section per unit area identified by modified Buffon method.

$$B_A = \frac{\sum_{j=1}^{n} B_j(str)}{\sum_{j=1}^{n} A_j(obj)} \qquad (16a)$$

It means that in this case we would use combination of test system of lines and points, the same as for identification of curve length in 2D (see Fig. 11, 14). If we substitute for the ratio $B_j(str)/ A_j(obj)$, then the formula 16 has following expression:

$$est(S(str)) = \frac{4}{p} \cdot B_A(str) \cdot V(obj) \qquad (16b)$$

Then we can substitute B_A for the known parameters from the formula 5 and in practice we will use the following equation:

$$est(S(str)) = 2 \cdot \frac{p}{l} \cdot \frac{\sum_{j=1}^{n} I_j(str)}{\sum_{j=1}^{n} P_j(obj)} \cdot V(obj) \qquad (16c)$$

where p/l is the number of test points divided by the actual length of the corresponding test lines in the test system used (constant for the given test system), n is the number of examined sections generated by the orientator, $I_j\ (str)$ is the number of intersection points between the studied curves and test lines, $P_j\ (obj)$ is the number of test points falling in the j-th section of the object and $V(obj)$ (mm^3) is the object volume (to estimate this parameter see section 2.4.).

2.6.2.3. Estimation of length of 3D curve using orientator

The method of orientator can be also used for the estimation of the length of 3-dimensional curves ($L(curve)$) or tubular structures such as fibres or vessels:

$$est(L(curve)) = 2 \cdot \frac{\sum_{j=1}^{n} Q_j(curve)}{\sum_{j=1}^{n} A_j(obj)} \cdot V(obj) \qquad (17)$$

where n is the number of examined sections generated by the orientator, $Q_j(curve)$ (j=1,...,n) is the number of the intersections between the curves (tubules, fibres) and the j-th section, $A_j(obj)$ is the area of the j-th section of the object comprising the curves and $V(obj)$ (mm^3) is the object volume. $Q_j(curve)$ is determined by counting the structures studied in the unbiased sampling frames. Area will determined by using point counting method (formula 3). Thus, in this case we would use a combination of unbiased sampling frame with point test system (see Fig. 18) systematically superimposed on a section (see Fig. 28). The length of studied curve can be estimated by following formula:

$$est(L(curve)) = 2 \cdot \frac{p}{a'} \cdot \frac{\sum_{j=1}^{n} Q_j(curve)}{\sum_{j=1}^{n} P_j(obj)} \cdot V(obj) \qquad (17a)$$

where n is the total number of sampling frames used $Q_j(curve)$ is the number of curve profiles sampled by the j-th unbiased sampling frame, p is number of test points belonging to one frame (4 in Fig. 18), a' (μm^2) is the (actual) area of the sampling frame obtained by calibration, $P_j(obj)$ is the number of test points of the p-point grid in the j-th frame hitting the object, $V(obj)$ is the object volume.

Another, sometimes more useful method of the estimation of the curve length in 3-D was described by Gokhale (1990). His idea was also exploited in the method of total vertical projections estimating the length of a bounded curve which is described in section 2.7. Recently, a length estimation method of 'global spatial sampling' using virtual test planes, analogous to the fakir method described below, in Section 2.6.4., was described (Larsen et al., 1998).

2.6.3. Spatial grid method

The spatial grid method as proposed by Sandau (1987) is a stereological method for estimating surface area based on interactive counting of intersections between the surface and a spatial grid of lines consisting of three perpendicular sets of equidistant parallel lines intersecting in knots of the grid (Fig. 35).

The practical implementation consists of superimposing a square or rectangular net on serial sections of a stack of perfectly registered sections consecutively and counting

intersection points of the surface with the line grids parallel to x-, y-, and z-axis. The surface area (S) can be estimated by:

$$estS = \frac{2}{3} \cdot (I_x d_y d_z + I_y d_x d_z + I_z d_x d_y) \quad , \tag{18}$$

where d_x , d_y , d_z are distances between neighboring parallel lines of the grid in the direction of the x-, y-, and z-axis, respectively, and I_x , I_y , I_z are numbers of intersection points of the surface with the line grids parallel to x-, y-, and z-axis, respectively.

In general, to get an unbiased estimate of the surface area by Sandau method, it is necessary to ensure an isotropic orientation of the spatial grid. It means that the serial sections should be cut at random, in an isotropic direction with respect to the surface.

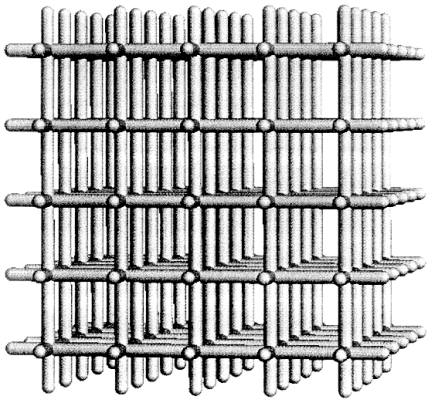

Fig. 35: Sandau spatial grid
Test lines are replaced by pipes here.

2.6.4. Fakir method

The fakir probe is a systematic probe consisting of parallel test lines (resembling nails of a fakir bed piercing the surface, see Cruz-Orive, 1993, and Fig. 36). Thus, Sandau spatial grid consists of three fakir probes (Fig. 35). When estimating the surface area, the intersections between the surface and the fakir probe are counted (Kubínová and Janácek, 1998). If a cubic spatial grid consisting of three mutually perpendicular fakir probes, halfway shifted with respect to each other (see Fig. 37), which has been proved to be highly efficient, is used, the surface area (S) can be estimated by the following formula:

$$estS = \frac{2}{3} \cdot u^2 \cdot (I_1 + I_2 + I_3) \tag{19}$$

where u is the grid constant (i.e. distance between neighboring parallel lines of the grid) and I_i (i=1,2,3) is the number of intersections between the surface and the i-th probe. The estimator (2) of the surface area is unbiased if the orientation of the spatial grid is isotropic.

This type of measurement can be easily performed if digitized images of series of perfectly registered sections of the surface are available and interactive FAKIR software is applied (see Kubínová and Janácek, 1998, available for free at http://www.biomed.cas.cz/fgu/fakir/3dtools.htm). This software generates an isotropic set of fakir probes and so it is not necessary to randomize the direction of the stack of sections. The object surface area is proportional to the number of intersection points between the object surface and the probe.

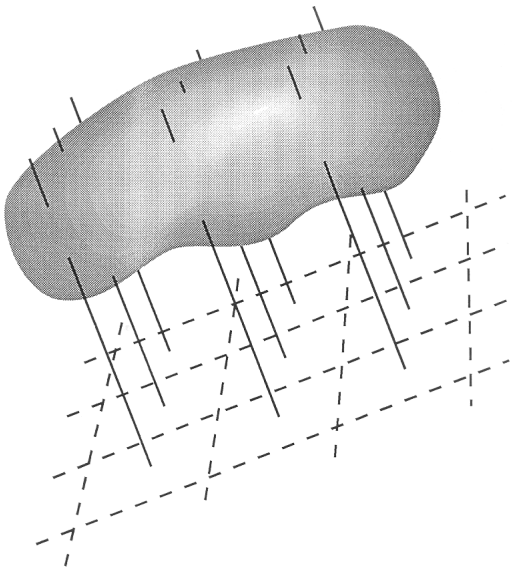

Fig.37: Orthogonal triplet of shifted fakir probes

A cubic spatial grid consisting of three mutually perpendicular fakir probes, halfway shifted with respect to each other which has been proved to be highly efficient (Kubínová and Janácek 1998). Test lines are replaced by pipes here.

Fig.36: The fakir probe (named by Cruz-Orive, 1993).

It is a systematic probe consisting of parallel test lines (resembling nails of a fakir bed piercing the surface. When estimating the fibre surface area, the intersections between the fibre surface and the fakir probe are counted.

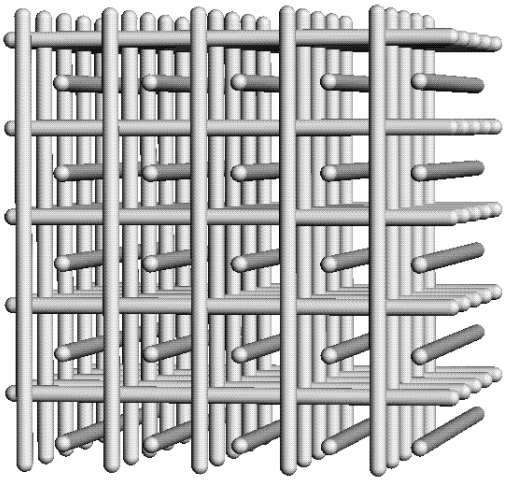

2.7. Estimation of the length of a bounded curve in 3-D using total vertical projections

The estimation of the curve length using total vertical projections (Cruz-Orive & Howard, 1991, Roberts et al., 1991) is based on counting the intersections between the vertical projection of the curve and a cycloid test system superimposed on the projection. The only requirements of the method are that the curve is rigid (i.e. of a constant shape) and that it is not too densely entangled so that the overlapping effects are negligible after projection. For example, if estimating the length of the root system by this method, the roots must not be too entangled and they must be embedded in a transparent medium such as water solution or air.

When using the method of total vertical projections, at first a convenient vertical axis is fixed with respect to the object under study - in the case the length measurements of the root system it might be the axis of the main root (see Albrechtová et al., 1997/98). Then, with a random starting position and continuing at uniform intervals, the whole object is projected onto a plane (e.g. by photographing) in a systematic set of directions between 0° and 180°, all perpendicular to the vertical axis (see Fig. 38). On each vertical projection, a cycloidal test system (Fig. 38B, Fig. 39) is superimposed with a uniform random position and with the shorter principal axes of the cycloids always perpendicular to the fixed vertical direction.

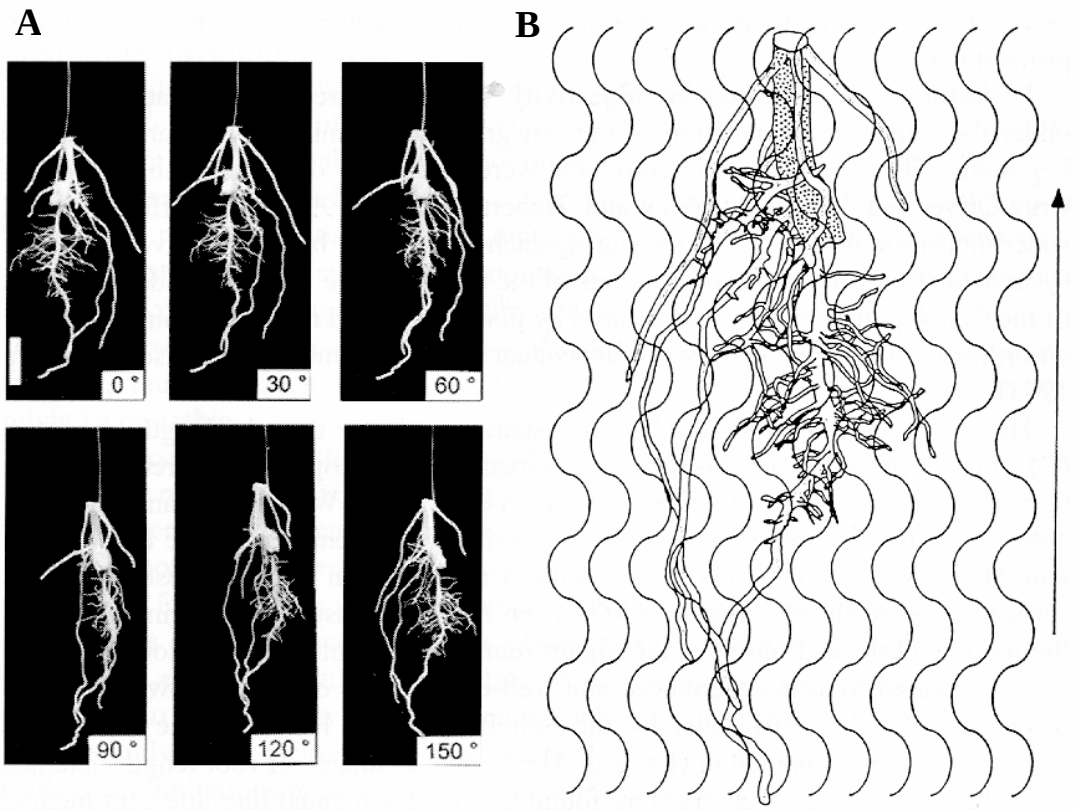

Fig. 38. Measurement of length of rigid root systems using method of total vertical projections

A) Six vertical projections of the root system of *Zea mays* taken under 30°-intervals of rotation. Before projections were root system was fixed in FAA what caused its rigid structure (for details see Albrechtová et al. 1997/98). The arrangement of the root system does not exhibit planar anisotropy. Scale = 2 cm.

B) Random superimposition of the cycloid test system on the root projection. Dotted area (caryopsis and mesocotyl) is not included into the measurement. The vertical direction is indicated by the arrow.

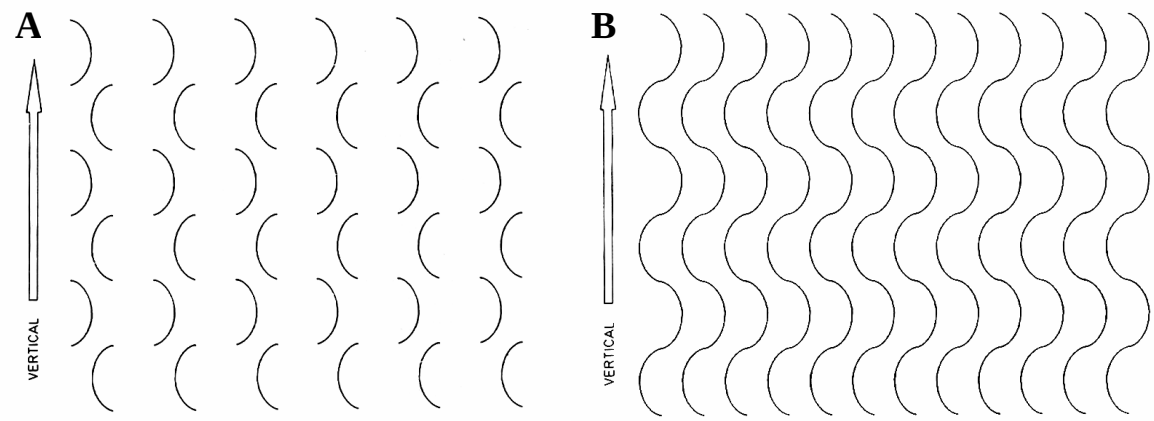

Fig.39: Cycloid test systems for estimating the length of a curve in 3-D.

A) The length of an isolated cycloid arc from the test system is four times its shorter (horizontal) axis (i.e. twice its height - see Fig.29B). For this test system a/l(cyc) equals p times the length of a short cycloid axis divided by the magnification used.

B) In the upper test system the test length per unit area is exactly twice that for the lower test system, so that a/l(cyc) is half of that for the lower test system.
(From Roberts et al., 1991.)

Intersections between the curves of each vertical projection and cycloid test lines are counted and the following unbiased estimator of curve length *L(curve)* is used:

$$estL(curve) = 2 \cdot \frac{a}{l(cyc)} \cdot \frac{1}{n} \sum_{j=1}^{n} I_j \qquad (20)$$

where *a/l(cyc)* is the ratio of test area to the actual cycloid test length, *n* is the number of vertical sections analysed and I_j (j=1,...,n) is the total number of intersections counted for the j-th projection.

2.8. Point-sampled intercepts method - estimation of volume-weighted mean volume

When measuring particle sizes two different ways of sampling particles are used in stereology. One way is to sample particles with identical probabilities - this kind of sampling is made using the disector (see section 2.5) and it results in the estimation of the mean particle volume in the ordinary sense, defined as the ratio of total particle volume to total particle number.

The second way is to sample particles with a probability proportional to the particle volume (i.e. larger particles are more likely to be sampled) which results in the estimation of the volume-weighted mean particle volume $\bar{v}_v(par)$. In this case the particle is sampled if it is hit by a test point of a point test system. This kind of sampling is used in the point-sampled intercepts method (Gundersen & Jensen, 1985) which leads to the estimation of $\bar{v}_v(par)$. The principle of this method is shown below in the case of quantifying the population of convex cells (i.e. cells having no protuberances or, more precisely, such cells that a straight line connecting any two arbitrary points inside the cell is lying entirely inside the cell). For the modification of the method for non-convex particles see Gundersen & Jensen (1985).

Consider a convex cell of an unknown volume ($v(cell)$) and take a uniform random point inside the cell. Independently, choose an isotropic random direction in space and draw a parallel line through the point. The resulting intercept (which is called a point-sampled intercept) is a connected segment of length l_0 (see Fig.40). Then $(p/3)\ l_0^3$ is an unbiased estimator of the cell volume.

Consider now a population of convex cells hit by a uniform random point (for its construction see below). The probability that a cell of volume $v(cell)$ is hit by a point is proportional to $v(cell)$ itself, and so the mean volume of hit cells is the volume-weighted mean cell volume ($\bar{v}_v(cell)$). Now, since the volume of a point-sampled cell can be estimated by the length of a corresponding point-

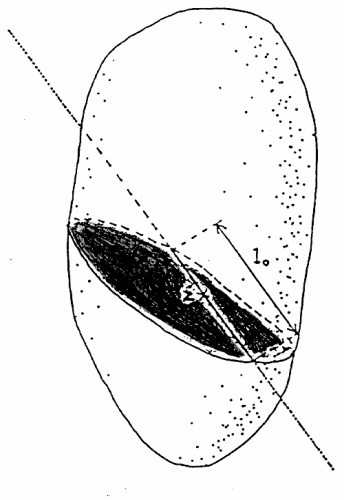

Fig.40: Point-sampled intercepts method.
(z) = uniform random point inside the cell;
(l_0) = the length of point-sampled intercept.

sampled intercept of it, as mentioned above, it follows that $\bar{v}_v(cell)$ can be estimated by the formula:

$$est(\bar{v}_V(cell)) = \frac{p}{3} \cdot \overline{l_0^3} \qquad (21)$$

where the average of the third power of observed point-sampled intercept lengths is counted.

In practice, we take a uniform random plane section with isotropic orientation with respect to the cells (it can be generated, e.g., by the orientator - see section 2.6.2). A grid of test points is superimposed on the section, and whenever a test point hits a cell transect, the corresponding point-sampled intercept is drawn through the transect (see Fig.41). The length l_0 of each point-sampled intercept is measured and formula (21) used. The vertical sections (see section 2.6.1) can also be used, only the orientation of intercepts must be constructed in a special way (see, e.g., Cruz-Orive & Hunziker, 1986).

Fig.41. Convex cells hit by a section plane with a grid of test points and associated directions.
Only cells hit by test-points are sampled
- and if a cell is hit by more than one test-point it is sampled more than once.

(l_0) = the length of point-sampled intercept.

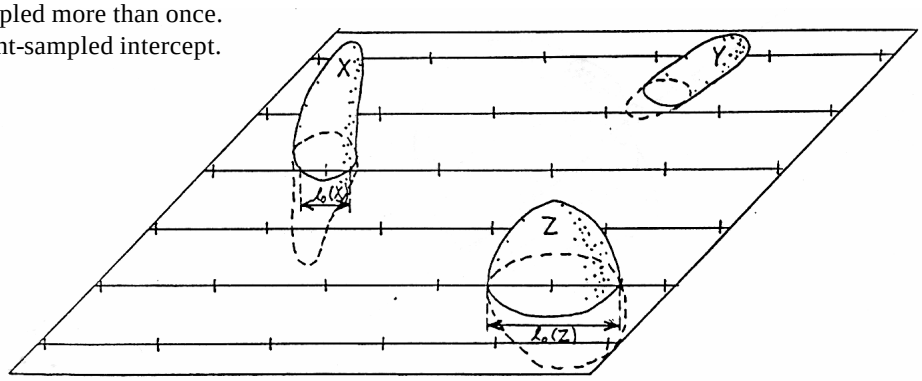

Fig.42: l_0 - ruler used for the direct measurement of l_0.

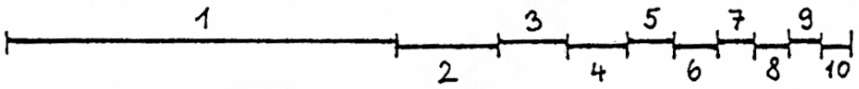

For the measurement of l_0^3 it is convenient to use a special ruler - l_0^3-ruler (Gundersen & Jensen, 1985). This ruler is constructed so that the intercepts are classified in n size classes on a scale equidistant in (length)^3 (see Fig.42), i.e. the cube root $\sqrt{j}$ of the integers j=1,2,...,n is used on the ruler as the right-hand limit of the j-th class. The ruler length L_n, i.e. the measured distance from the left-hand limit of class 1 to the right-hand limit of class n, is chosen so that in the specimen under study one does not encounter an intercept longer than L_n. The average of the third power of observed point-sampled intercept lengths is then calculated:

$$\overline{l_0^3} = \frac{1}{m} \cdot \frac{L_n^3}{n \cdot M^3} \cdot \sum_{j=1}^{n} (m_j (j - \tfrac{1}{2})) \qquad (22)$$

where M is the magnification used, m_j (j=1,...,n) is the number of intercepts falling within the j-th interval, and m is the number of measured intercepts (i.e. $m = m_1 + m_2 + ... + m_n$).

The practical implementation of l_0^3- ruler is shown in Fig.43.

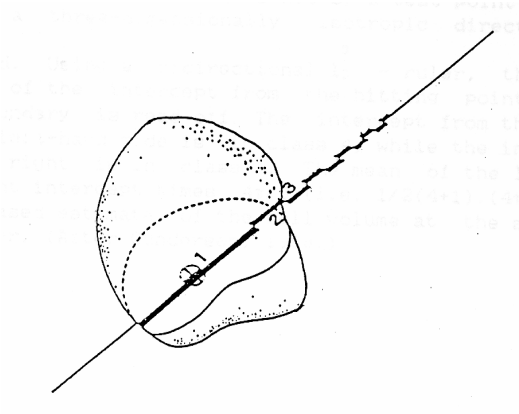

Fig.43. Using the l_0 - ruler for determining l_0 for a convex cell hit by a sample point with an associated direction.

The class number of the intercept length through the sample point is read off, i.e. j = 2 here. (After Gundersen and Jensen, 1985.)

2.9. Selector and nucleator - estimation of mean cell volume

The methods of selector (Cruz-Orive, 1987) and nucleator (Gundersen, 1988) leading to the estimation of the ordinary mean particle volume $v(par)$ will be briefly described (see also Cruz-Orive & Weibel, 1990).

Both methods require, in general, an isotropic stack of serial sections from samples taken from the object under study. It is necessary to identify each particle in each section of the stack - this requirement can cause some technical difficulties. Two of the planes of the stack are used to make a disector (see section 2.5) which samples some of the particles. The nucleator is suitable for cells with a single nucleus (or even nucleolus), in which case a cell is sampled only if its nucleus (or nucleolus) is sampled by the disector. If the particles under study do not exhibit any single, internal core, then the selector may be used. In both methods, the disector thickness need not be known.

Once a sample of particles is available, the volume of each of them must be estimated. Since all particles were sampled with equal chances with disectors, the arithmetic mean of the volume estimates is an unbiased estimate of the mean particle volume $\bar{v}(par)$.

The sampling requirements for the nucleator principle in its standard implementation for cells with one nucleus of convex shape (i.e. nucleus having no protuberances or, more precisely, having the property that a straight line connecting any two arbitrary points inside the nucleus is lying entirely inside the nucleus) are described below (Gundersen, 1988):

1) Make a small series of sections of unknown thickness with uniform random position in the reference space. The stack of sections must have either isotropic or vertical orientation distribution and the stack must be higher than any one nucleus. (For example, in the case of leaf mesophyll cells with visibly stained nucleus, the vertical sections or isotropic sections are generated as described in 2.6.1.)
2) Using the second section in the stack as the lower section of the disector, sample all nuclei not hit by the first 'look-up' section (see section 2.5.).
3) Place a systematic set of points at random on the second section in the stack and all the following sections where the sampled nuclei are seen. Select a three-dimensionally isotropic direction, preferentially one per cell to be measured or one per field of vision. Whenever a point hits one of the sampled nuclei the distances from the point to the cell boundary in the selected direction and

in the opposite direction (Fig.29) are measured. If the nucleus is hit only by one test point (in all its sections) take the average of these two cubed distances. If the nucleus, say the *j*-th, is hit by more test points calculate the simple mean of all the cubed distances through it and denote it l_j^3(nuc). Any sampled nucleus must be hit at least once by a test point. If not, superimpose the points on all sections through the nucleus again.

4) Averaging over all the *m* sampled nuclei, the relationship

$$est(\bar{v}(cell)) = \frac{4p}{3} \cdot \frac{1}{m} \cdot \sum_{j=1}^{m} l_j^3(nuc) \qquad (23)$$

provides an unbiased estimate of the ordinary mean cell volume. For the procedure in the case of non-convex shape of nuclei see Gundersen (1988).

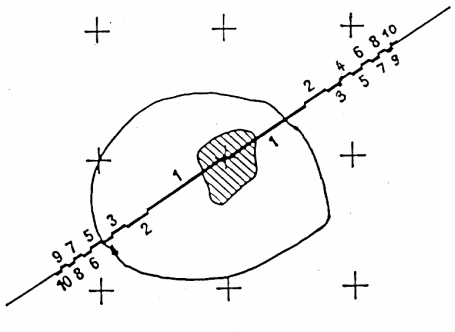

Fig. 44. The nucleator.
A disector-sampled nucleus is hit by a test point through which a three-dimensionally isotropic direction is selected. Using a bidirectional l_0 - ruler, the class number of the intercept from the hitting point to the cell boundary is read off. The intercept from the point to the left-hand side is in class 4, while the intercept to the right is in class 1. The mean of the left and the right intercept times 4p/3, i.e. 0.5 x (4+1) x (4p/3), is an unbiased estimate of the cell volume at the scale of the ruler. (After Gundersen, 1988.)

When using the selector principle (Cruz-Orive, 1987), the sampling requirements are analogous to those described in paragraphs (1), (2), and (3), only whole cells instead of the nuclei are treated and cubed length of point-sampled intercepts (l_0^3) are measured (i.e. direction from one particle boundary to the other, see section 2.8.). The mean cell volume is then estimated:

$$est(\bar{v}(cell)) = \frac{p}{3} \cdot \overline{l_0^3} \qquad (24)$$

For details and for the procedure in the case of non-convex particles see Cruz-Orive (1987).

Using the nucleator or selector method together with the point-sampled intercept method (section II.8.) the coefficient of variation of volume in the cell population ($CV_N(v)$) can be estimated because the following equation holds:

$$CV_N(v) = \sqrt{\left(\frac{\bar{v}_V(cell)}{\bar{v}(cell)} - 1 \right)} \qquad (25)$$

The coefficient of variation $CV_N(v)$ gives the information about the distribution of sizes of cells from the cell population under study.

3. Sampling design of a stereological experiment

When planning experiments using stereological methods it must be decided not only which structural characteristics will be measured and which stereological procedures will be used, but also how many plants and, e.g., leaves, how many sections per leaf, how many points or intersections, etc. should be considered in order to get sufficiently precise results. It should be mentioned here that a stereological project should be planned so that the required number of leaves per experimental group is assessed first, and the number of points or intersections last.

If comparing two different groups of individuals, the sampling design of the experiment in fact depends on variation among experimental groups (to remind you see Table 1), i.e the standard deviation of the estimate of the stereological parameter among individuals and the absolute mean difference we would like to detect between the groups. The smaller the variation between individuals and the larger the difference between the groups, the fewer individuals per group are required. When determining efficiency of our measurements a rigorous approach based on statistical treatment would be best to use. We strongly recommend to look in reference literature cited in this section (a good review is also given in a texbook on stereology by Howard and Reed, 1998). However, certain generalizations can be concluded about arrangement of our experiment (e.g Cruz Orive and Weibel, 1990), which will be presented below. Also preliminary experiment can reveal the mentioned variation between individuals and variance contributions of different sampling stages so that efficient sampling design can be developed (see, e.g., Michel and Cruz-Orive, 1988).

Table 1: Measures of variability. Variation of a parameter can be expressed by several generally accepted statistical characterstics, so we should not forget to include a proper abbreviation of statistical parameter.

(n is number of individuals in one group, x_i is value of a parameter for i-th individual in a group, $\bar{x}$ is the average value for a group)

Measure of variability	Calculation	Abbreviation
Variance	$= \frac{1}{n-1} \cdot \sum_{i=1}^{n} (x_i - \bar{x})^2$	var s^2 s^2
Standard deviation	$= v(\text{var})$	SD v(var) v(s^2) v(s^2)
Coefficient of variance	$= \frac{v(\text{var})}{\bar{x}}$	CV
Coefficient of error	$= \frac{v(\text{var})}{\bar{x} \cdot vn} = \frac{CV}{vn}$	CE

In many cases, taking five individuals per group might be a good starting point (Cruz-Orive and Weibel, 1990). Further, from five to ten segments or sections per organ will usually be sufficient. In most cases it will not be necessary to count more than 200 points or intersections per organ in each compartment of interest (Gundersen and Jensen, 1987).

The sampling probes should be designed so that they sample from 100 to 200 particles per organ. It is convenient to make the sampling frame small enough, so that it samples not more than 10 profiles. When using the disector principle, the estimation procedure is usually most efficient if the disector height is about a third or fourth of the mean particle height (Gundersen, 1986). It can also be recommended to increase the efficiency two times by using the disector both ways, i.e. using in turn any of its two sections as the sampling section and the other one as the look-up section (Gundersen, 1986, Fig.25).

4. Conclusive practical considerations

The sampling frames and point test systems can be placed in the ocular of the microscope or on the projection screen, on the micrograph of a structure under study or they can be generated by computer graphics and projected either into the field of vision of the microscope or on the screen of the monitor (Krekule and Gundersen, 1989). A computer-assisted approach can be very convenient (yet more expensive) if a special software for displaying the test system over the evaluated image is available, e.g. CAST-Grid (Olympus, Denmark), Digital Stereology (Kinetic Imaging Ltd, UK), STESYS (Karen et al., 1998) or Ellipse. The ocular test systems can be easily made according to our own choice (see section 1.1.6.).

The measurement of the disector height is discussed in detail in Gundersen (1986). In short, in the case of physical disector this measurement is based on measuring the section thickness. For the measurement of distances between optical planes it is recommended to use a microcator rather than the fine focus knob of the microscope.

In practical implementation of stereological methods it is necessary to take into account different types of errors which may occur due to the microtechnical processing of the material under study or due to other technical restrictions. One of these errors is caused by the tissue shrinkage during fixation, embedding and cutting of material. The tissue shrinkage is high especially in the case of embedding in paraffin (e.g., about 20% for area measurements in the sections of barley leaf - Kubínová, 1989) and it can result in the underestimation of volume, surface area and mean cell volume. However, the cell number estimated by the disector principle is not affected by tissue shrinkage (see Sterio, 1984). Another source of error stems from the fact that the examined sections are slices of certain positive thickness. This means that in fact we do not evaluate the intersection of a plane with the object (as it is assumed in the relevant stereological formulas) but a projection of a slice into a plane. In our botanical context it can result, e.g., in the underestimation of the proportion of intercellular spaces in the leaf. Finally, the sectioning process can cause truncation (minor, often peripheral parts of non-transparent material are not visible or not present in the section). The effect of finite section thickness (Weibel, 1979) and truncation are not present when counting cells with the disector (Sterio, 1984). On the other hand the mean cell volume can be affected by these errors.

It is difficult to quantify the mentioned errors and so we try to minimize them by technical means. All mentioned errors are much less pronounced if plastic embedding is used instead of paraffin embedding. The effect of section thickness can be reduced by making physical sections as thin as possible or, in light optics, by evaluating optical sections (inside the physical section) as thin as possible, using objective lenses with high numerical aperture or possibly a confocal microscope.

5. Literature cited

Albrechtová J, Kubínová L. 1991. Quantitative analysis of the structure of etiolated barley leaf using stereological methods. Journal of Experimental Botany 42, 1311-14.

Albrechtová J, Kubínová L, Votrubová O, Eliášová K. 1997/98. Non-destructive stereological method for estimating the length of rigid root systems. Biologia Plantarum 40: 311-316.

Baddeley AJ, Gundersen HJG, Cruz-Orive LM. 1986. Estimation of surface area from vertical sections. Journal of Microscopy 142, 259-76.

Barba J, Chan KS, Gil J. 1992. Quantitative perimeter and area measurements of digital images. Microsc. Res. Tech. 21, 300-313.

Briarty LG. 1975. Stereology: Methods for quantitative light and electron microscopy. Science Progress (Oxford) 62, 1-32.

Charles-Edwards DA, Charles-Edwards J, Sant FI. 1972. Models for mesophyll cell arrangement in leaves of ryegrass (Lolium perenne L.). Planta 104, 297-305.

Cochran WG. 1977. Sampling Techniques. New York: Wiley.

Cruz-Orive LM. 1987. Particle number can be estimated using a disector of unknown thickness: the selector. Journal of Microscopy 145, 121-42.

Cruz-Orive LM. 1993. Systematic sampling in stereology. Bull. Intern. Statis. Inst. Proceedings 49th Session, Florence 1993, 55(2), 451-468.

Cruz-Orive LM, Howard CV. 1991. Estimating the length of a bounded curve in three dimensions using total vertical projections. Journal of Microscopy 163, 101-113.

Cruz-Orive LM, Howard CV. 1995. Estimation of individual feature surface area with the vertical spatial grid. Journal of Microscopy 178, 146-151.

Cruz-Orive LM, Hunziker EB. 1986. Stereology for anisotropic cells: application to growth cartilage. Journal of Microscopy 143, 47-80.

Cruz-Orive LM, Weibel ER. 1990. Recent stereological methods for cell biology: a brief survey. American Journal of Physiology 258, L148-L156.

Dengler NG, MacKay LB. 1975. The leaf anatomy of beech, Fagus grandifolia. Canadian Journal of Botany 53, 2202-11.

El-Sharkawy M, Hesketh J. 1965. Photosynthesis among species in relation to characteristics of leaf anatomy and CO_2 diffusion resistances. Crop Science 5, 517-21.

Gokhale AM. 1990. Unbiased estimation of curve length in 3-D using vertical slices. Journal of Microscopy 159, 133-141.

Gundersen HJG. 1977. Notes on the estimation of the numerical density of arbitrary profiles: the edge effect. Journal of Microscopy 111, 219-23.

Gundersen HJG. 1988. The nucleator. Journal of Microscopy 151, 3-21.

Gundersen HJG. 1986. Stereology of arbitrary particles. A review of unbiased number and size estimators and the presentation of some new ones, in memory of William R. Thompson. Journal of Microscopy 143, 3-45.

Gundersen HJG, Bagger P, Bendtsen TF et al. 1988a. The new stereological tools: Disector, fractionator, nucleator and point sampled intercepts and their use in pathological research and diagnosis. APMIS 96, 857-881.

Gundersen HJG, Bendtsen TF, Korbo L et al. 1988b. Some new, simple and efficient stereological methods and their use in pathological research and diagnosis. APMIS 96, 379-394.

Gundersen HJG, Boysen M, Reith A. 1981. Comparison of semiautomatic digitizer-tablet and simple point counting performance in morphometry. Virchows Archiv (Cell Pathol) 37, 317-325.

Gundersen HJG, Jensen EB. 1985. Stereological estimation of the volume-weighted mean volume of arbitrary particles observed on random sections. Journal of Microscopy 138, 127-142.

Gundersen HJG, Jensen EB. 1987. The efficiency of systematic sampling in stereology and its prediction. Journal of Microscopy 147, 229-63.

Harris PJ, Lowry KH, Chapas LC. 1981. Comparison of methods for measuring tissue areas in sections of plant organs. Annals of Botany 47, 151-154.

Howard CV, Reed MG. 1998. Unbiased Stereology. BIOS Scientific Publishers - Oxford.

Karen P, Kubínová L, Krekule I. 1998. STESYS software for computer-assisted stereology. Physiological Research 47, 271-278.

Krekule I, Gundersen HJG. 1989. Computer graphics enhancement of measurements in stereology. Acta Stereologica 8, 533-5.

Kubínová L. 1989. Stereological analysis of the leaf of barley. Acta Stereologica 8, 19-26.

Kubínová L. 1991. Stomata and mesophyll characteristics of barley leaf as affected by light: Stereological analysis. Journal of Experimental Botany 42, 995-1001.

Kubínová L. 1993. Recent stereological methods for the measurement of leaf anatomical characteristics: Estimation of volume density, volume and surface area. Journal of Experimental Botany 44, 165-73.

Kubínová L. 1994. Recent stereological methods for measuring leaf anatomical characteristics: Estimation of the number and sizes of stomata and mesophyll cells. Journal of Experimental Botany 45, 119-127.

Kubínová L. 1998. Stereology in plant anatomy: Application of recent stereological principles to evaluation of plant cells. Folia Anatomica 26 (Suppl.1), 1-7.

Kubínová L, Janácek J. 1998. Estimating surface area by the isotropic fakir method from thick slices cut in an arbitrary direction. Journal of Microscopy 191, 201-211.

Larsen JO, Gundersen HJG, Nielsen J. 1998. Global spatial sampling with isotropic virtual planes: estimators of length density and total length in thick, arbitrarily orientated sections. Journal of Microscopy 191, 238-248.

Mathieu OL, Cruz-Orive LM, Hoppeler H, Weibel ER. 1981. Measuring error and sampling variation in stereology: comparison of the efficiency of various methods for planar image analysis. Journal of Microscopy 121, 75-88.

Mattfeldt T, Mall G, Gharehbaghi H, Möller P. 1990. Estimation of surface area and length with the orientator. Journal of Microscopy 159, 301-17.

Michel RP, Cruz-Orive LM. 1988. Application of the Cavalieri principle and vertical sections method to lung: estimation of volume and pleural surface area. Journal of Microscopy 150, 117-36.

Parker ML, Ford MA. 1982. The structure of the mesophyll of flag leaves in three Triticum species. Annals of Botany 49, 165-76.

Parkhurst DF. 1982. Stereological methods for measuring internal leaf structure variables. American Journal of Botany 69, 31-9.

Pazourek J. 1966. Anatomical gradients. Acta Universitatis Carolinae - Biologica, Suppl. 1/2, 19-25.

Pyke KA, Marrison JL, Leech RM. 1991. Temporal and spatial development of the cells of the expanding first leaf of Arabidopsis thaliana (L.) Heynh. Journal of Experimental Botany 42, 1407-1416.

Roberts N, Howard CV, Cruz-Orive LM, Edwards RHT. 1991. The application of total vertical projections for the unbiased estimation of the length of blood vessels and other structures by magnetic resonance imaging. Magnetic Resonance Imaging 9, 917-925.

Sandau K. 1987. How to estimate the area of a surface using a spatial grid. Acta Stereologica 6, 31-36.

Slavík B. 1963. The distribution pattern of transpiration rate, water saturation deficit, stomata number and size, photosynthetic and respiration rate in the area of the tobacco leaf blade. Biologia Plantarum 5, 143-53.

Sterio DC. 1984. The unbiased estimation of number and sizes of arbitrary particles using the disector. Journal of Microscopy 134, 127-36.

Toth R. 1982. An introduction to morphometric cytology and its application to botanical research. American Journal of Botany 69, 1694-1706.

Turrell FM. 1936. The area of the internal exposed surface of dicotyledon leaves. American Journal of Botany 23, 255-64.

Weibel ER. 1979. Stereological methods, Vol 1. Practical methods for biological morphometry. Academic Press.

6. Matrixes for stereological grids

A) Point counting method: area belonging to 1 point of the test grid a=5 x 5 mm^2

B) Area estimation in 2D (point counting method, linear integration method)
distance between 2 lines = distance between 2 points = 7mm

C) Modified Buffon method (density of curve length per area unit):
combination of line test system and point counting grid
length of 1 segment l = 10mm,
number of points per 1 segment p = 2 (without marginal points of segments)
area a belonging to 1 point of point test grid: a = 10 x 10 mm^2

D) Line-intercept method (Buffon method - curve length in 2D):
combination of isotropic (circle arcs) and anisotropic (lines) test systems
length of 1 circle arc = length of size of 1 square = 6mm

E) Unbiased sampling frame (counting of particles in 2D) combined with 1 point:
(from Howard and Reed 1998)

F) Cycloid test system combined with unbiased sampling frame and point counting grid.
p/l (mm^{-1}) is the ratio of test point number (p=1 here) to cycloid arc (actual) length
(the length of a cycloid arc equals twice its height)

G) Unbiased sampling frames (counting of particles in 2D) combined with 1 point:
(from Howard and Reed 1998)

H) 11-class ruler

I) Cycloid test system
length of 1 circle arc is 6.5mm

A)

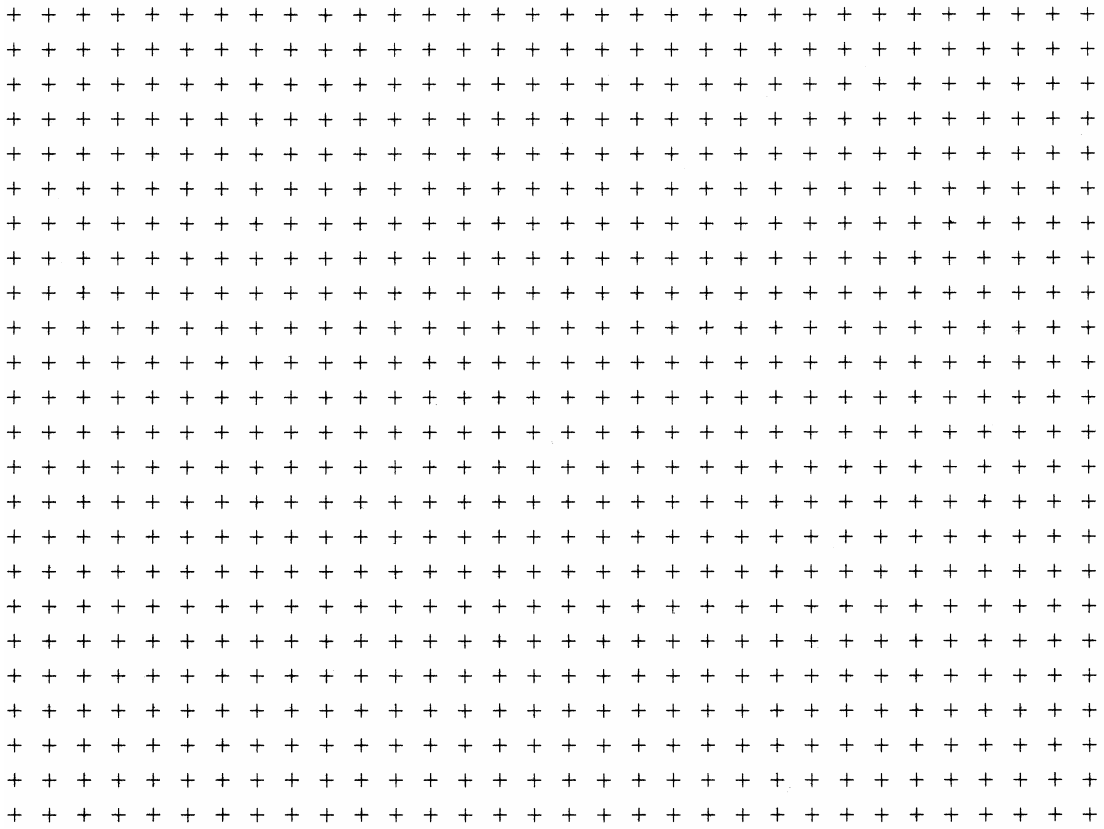

B)

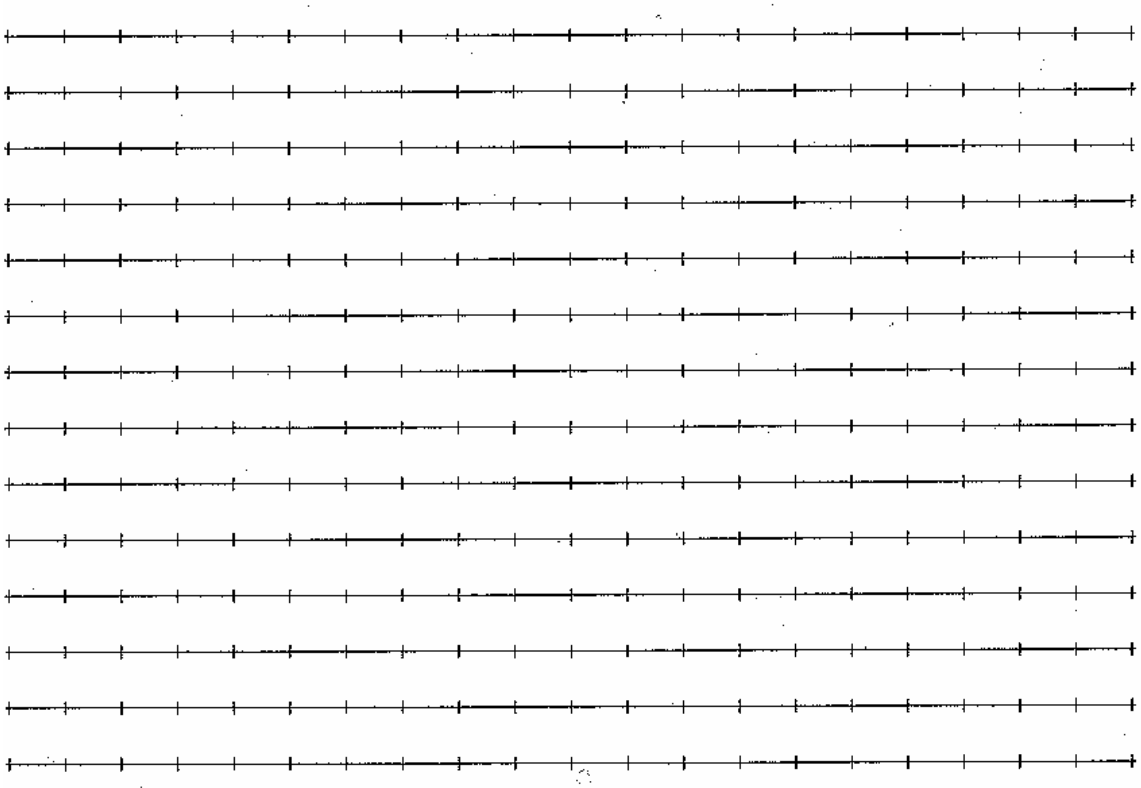

C)

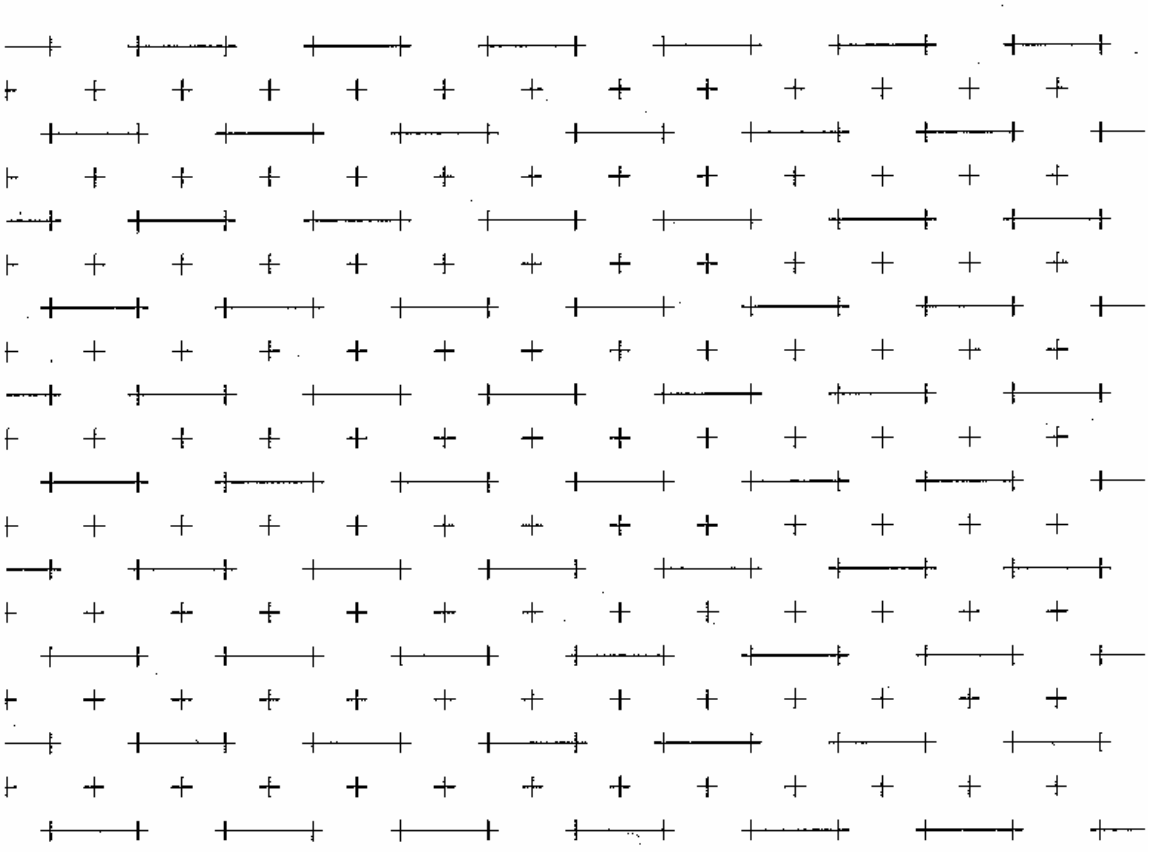

D)

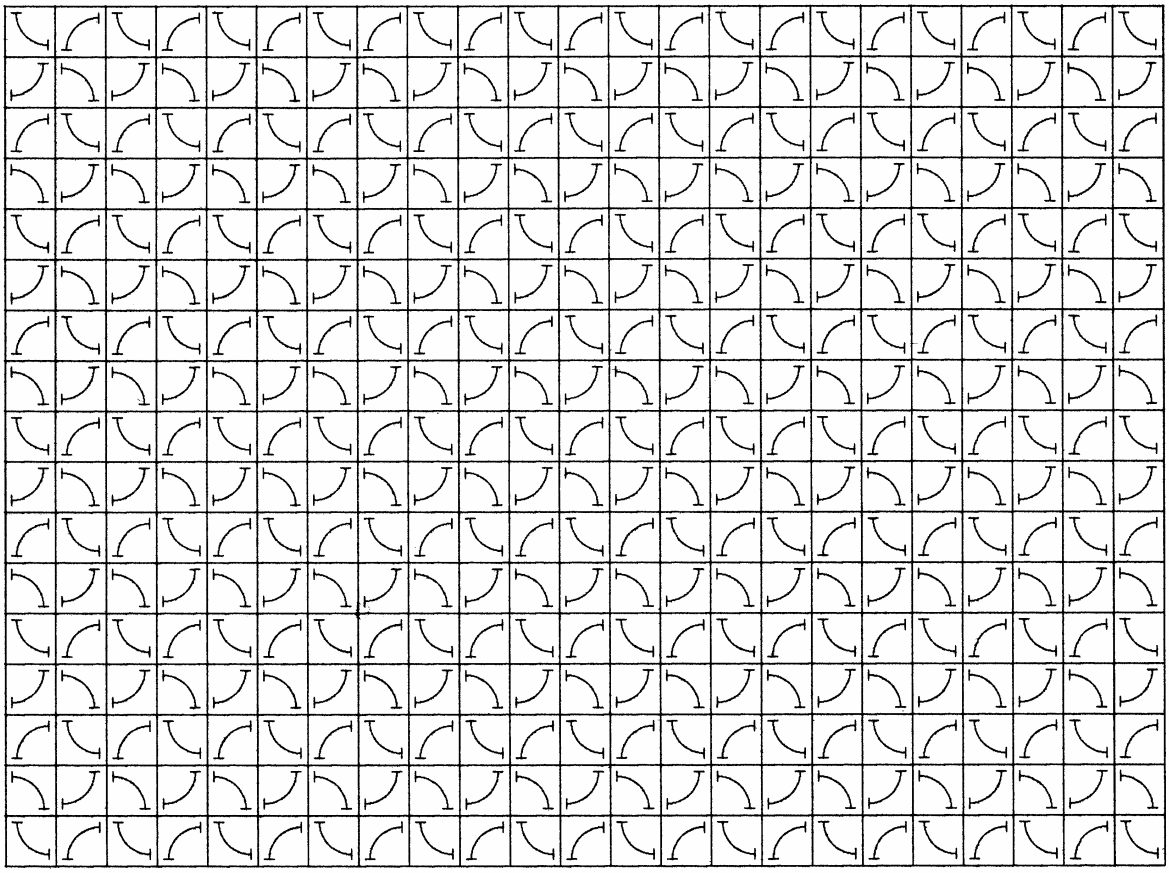

E)

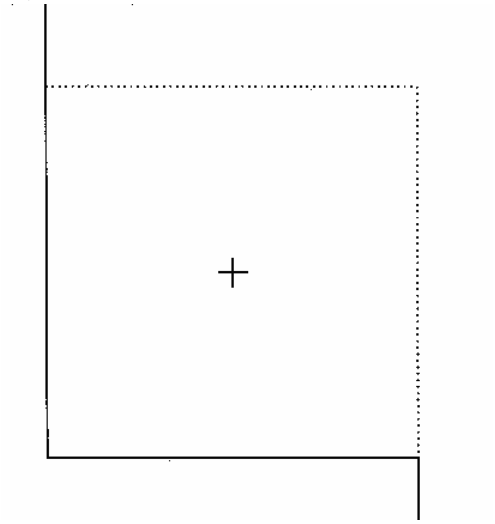

F)

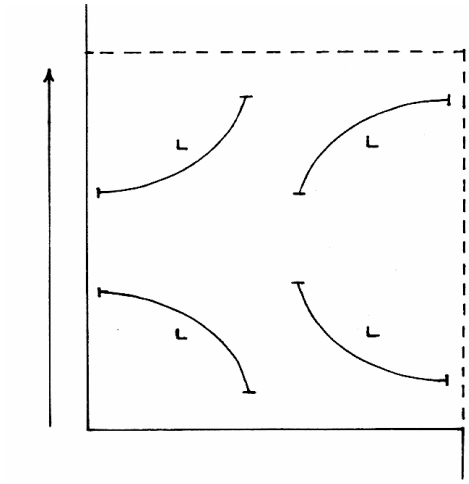

G)

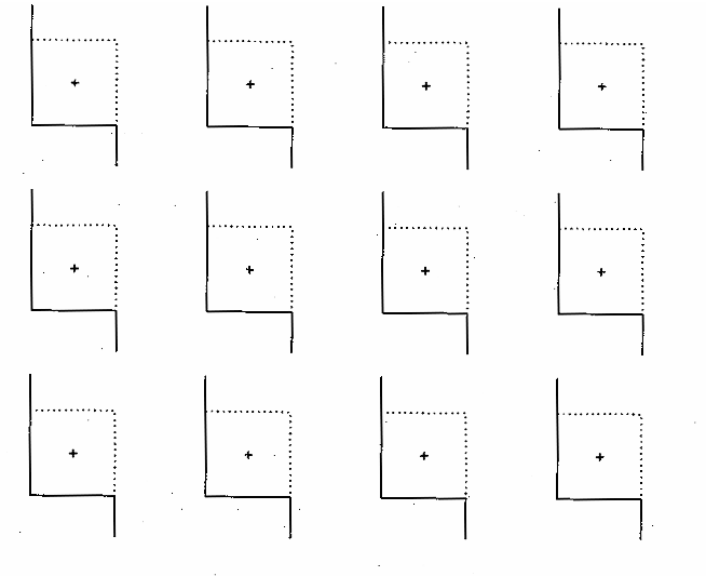

H)

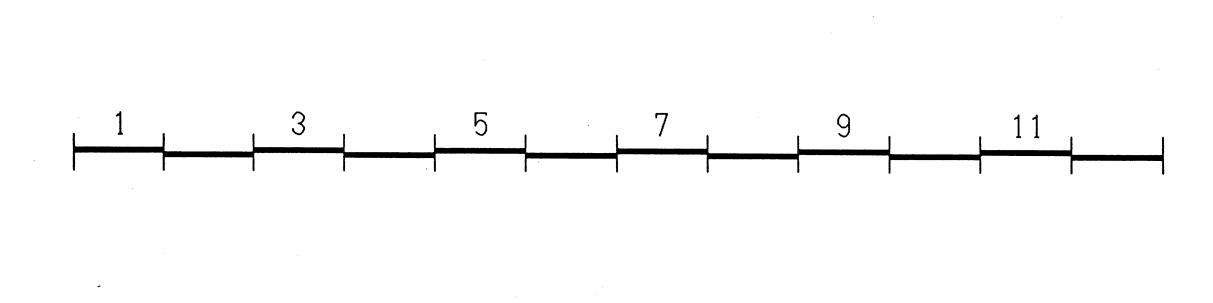

I)